Theoretical Papers

90/2005

Title: A comparison of methods for modeling quantitative structure-activity relationships.

Authors: Sutherland, J. J.; O'Brien, L. A.; Weaver*, D. F.
Departments of Medicine (Neurology) and Chemistry and School of Biomedical Engineering, Dalhousie University
Halifax, Nova Scotia B3H 4J3, Canada.
E-mail: weaver@chem3.chem.dal.ca; Tel.: 1-902-494-7183; Fax: 1-902-494-1310.

Source: J. Med. Chem. 2004, 47(22), 5541 – 5554.

Compounds: 114 ACE inhibitors, 111 AChE inhibitors, 163 BZR inhibitors, 322 COX-2 inhibitors, 397 DHFR inhibitors, 66 GPB inhibitors, 76 THER inhibitors, and 88 THR inhibitors.

Biological material: Angiotensin converting enzyme (ACE), acetylcholinesterase AChE), benzodiazepine receptor (BZR), cyclooxygenase-2 (COX-2), dihydrofolate reductase (DHFR), glycogen phosphorylase b (GPB), thermolysin (THER), and thrombin (THR).

Data taken from the literature:

Datasets [datasets of inhibitors for ACE, AChE, BZR, COX-2, DHFR, GPB, THER, and THR with K_i and/or IC_{50} enzyme affinity data (details not given)].

Computational methods:

ComFA [Comparative Molecular Field Analysis of the molecules was carried out represented by their steric and electrostatic fields sampled at the intersections of a three-dimensional lattice (2 Å grid increment) using an sp^3 carbon atom probe with a charge of +1, the regression analyses are done using PLS algorithms];

CoMSIA [Comparative Molecular Similarity Indices Analysis of the molecules was carried out as an alternative approach to CoMFA based on similarity indices calculated at the intersections of a three dimensional lattice, the five physicochemical properties for CoMSIA (steric, electrostatic, hydrophobic, and hydrogen bond donor and acceptor) were evaluated];

HQSAR (Hologram QSAR, a novel program correlating molecular structure with biological activity for a set of compounds using molecular holograms constructed from counts of substructural fragments of the molecules);

EVA [infrared range vibration based theoretical descriptor derived by processing the normal coordinate frequencies for each molecule by projecting the eigenvalues (normal coordinate frequencies) onto a bounded frequency scale of 0–4000 cm^{-1}, each vibration on this scale had Gaussian curve superimposed on it to produce a summed intensity, the program Spectrum is used to sample the resulting spectrum];

PLS (Partial Least Squares projections to latent structures analysis methodology including genetic PLS);

GFA (Genetic Function Approximation for the generation of multiple QSAR models by evolving random initial models using a genetic algorithm);

CNN (back-propagation Computational Neural Networks implemented in Cerius2);

LOO (Leave-One-Out cross-validation).

Data calculated:

Descriptors (descriptors were calculated with CoMFA, CoMSIA, EVA, HQSAR, and traditional 2D and 2.5D descriptors were computed from CORINA structures and Gasteiger-Marsili charges).

Results: A comparative study of methods for modeling quantitative structure-activity relationships has been performed using descriptors calculated with CoMFA, CoMSIA, HQSAR, EVA and traditional 2D and 2.5D descriptors and methods, and in addition GFA, genetic PLS, and back-propagation NN methodologies. The predictive accuracy of these methods was examined using designed test sets of inhibitors for ACE, AChE, BZR, COX-2, DHFR, GPB THER, and THR. For virtual screening applications HQSAR proved to be the most promising of the approaches examined. Field-based 3D QSAR methods were found to be the most predictive for extrapolating outside the training set. When 2.5D descriptors were used, only CNN ensembles were found to be similarly or more predictive than PLS models. In addition, it was shown that many cross-validation procedures yielded similar estimates of the interpolative accuracy of methods. The lack of correspondence between cross-validated and test set predictive accuracy for four sets highlighted the advantage of using designed test sets. Only those methods were examined which are available in commercial software packages. There are many approaches that have been described in the literature that appear very predictive while overcoming limitations of established methods (e.g., CoMMA, MS-WHIM, 4D-QSAR, Quasar, PharmPrint, GRIND, etc.).
(B. B.)

91/2005

Title: MIA-QSAR. A simple 2D image-based approach for quantitative structure-activity relationship analysis.

Authors: Freitas, M. P.; Brown, S. D.; Martins*, J. A.
EMS Sigma Pharma
Rodovia SP 101 Km 08, Hortolândia, SP 13186 – 401, Brazil.
E-mail: jose.martins@ems.com.br; Tel.: 55-019-3887-9353; Fax: 55-019-3887-9889.

Source: J. Mol. Struct. 2005, 738(1 – 3), 149 – 154.

Compounds:

a) 58 Dompamine D2 ligands of type I, where R^1 = H, OH; R^2 = H, F, Cl, Br, I, Me, Et, OMe, n-Pr, SMe, n-Bu, NO_2; R^3 = H, F, Cl, Br, OMe, Me, n-Pr, Et, NO_2.

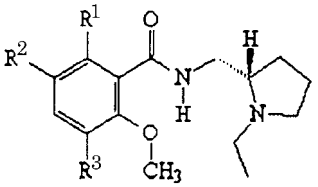

I

Biological material:

a) Dopamine D_2 receptor subtype;
b) HIV-1 protease (HIV PR), cyclooxygenase (COX-2), nAChR.

Data taken from the literature:

IC_{50} [concentration of the test substance required for 50% inhibition of the D2 receptor subtype (details not given)];

b) HIV PR inhibitors, cyclooxygenase (COX-2) inhibitors, nAChR ligands as well as anxiolytic agents) with biological data against their target.

Computational methods:

MIA-QSAR [Multivariate Image Analysis QSAR was performed as follows: 2D structures of each compound of type I were drawn in the ChemSketch module of ACDLabs program and saved in Paint Brush as bmp files, with resolution of 64×64 points per inch, the bitmap windows were cut to a 185 pixels $\times$ 143 pixels size to minimize memory and the drawn molecules were systematically fixed in a given coordinate by a common point among them, each image was unfolded to an $1 \times 26{,}455$ row and then the 58 images were grouped to form a calibration set matrix of $40 \times 26{,}455$ and a validation set matrix of $18 \times 26{,}455$, a calibration set matrix of $40 \times 12{,}727$ and a validation set matrix of $18 \times 12{,}727$ was constructed, bilinear (conventional) PLS was utilized as the regression method and leave-one-out cross-validation was performed to derive the QSAR model];

PLS (Partial Least Squares projections to latent structures analysis was performed using the NIPALS algorithm);

LOO (Leave-One-Out cross-validation).

Data calculated:

Descriptors [26455 descriptors generated using the MIA-QSAR methodology (details are given)];

SEE (Standard Error of Estimation);

SEP (Standard Error of Prediction);

q^2 (cross-validated correlation coefficient).

Results: A simple 2D image-based approach, MIA-QSAR, for quantitative structure-activity relationship analysis is presented. The performance of the method was demostrated by using a well known set of dopamine D_2 ligands of type I, which was divided in 40 calibration compounds and 18 test compounds and 26455 descriptors were generated from pixels of 2D structures of each compound, drawn with an appropriate program. Bilinear PLS was utilized as the regression method and LOO cross-validation was performed. The good predicted q^2 values were obtained for the sets compounds (model, r, q^2, s for calibration set, s for test set, SEE, SEP, F): model for the whole molecule, 0.94, 0.58, 0.16, 0.56, 0.03, 0.30, 726; model for the aromatic portion of the molecule, 0.95, 0.53, 0.17, 0.59, 0.03, 0.34, 750. Fig. 1 shows the plot of actual versus predicted pIC_{50} values of the calibration set (open squares) and test set (closed squares) compounds for the aromatic portion of the compounds.

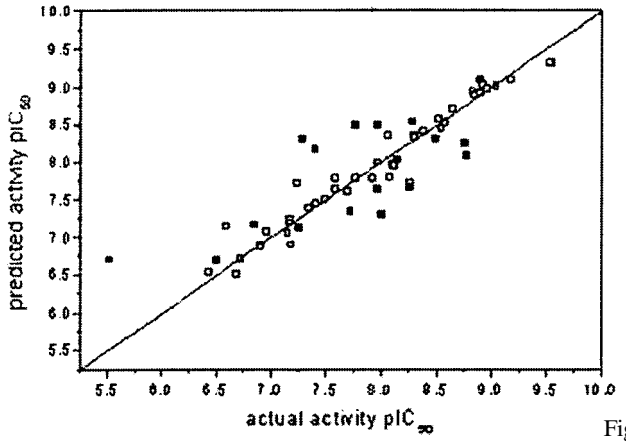

Fig. 1

In a comparative study using MIA-QSAR similar prediction capabilities were obtained for other data sets (nAChR ligands, HIV protease inhibitors, COX-2 inhibitors and anxiolytic agents), suggesting that the model is robust and has a comparable performance to other more complex methods. An advantage of the method is that the method does not need 3D alignment as it uses a 2D approach.
(B. B.)

92/2005

Title: A novel method of estimation of lipophilicity using distance-based topological indices. Dominating role of equalized electronegativity.

Authors: Agrawal, V. K.; Gupta, M.; Singh, J.; Khadikar, P. V.

Research Division, Laxmi Fumigation and Pest Control Pvt. Ltd

3 Khatipura, Indore 452 007, India.

E-mail: pvkhadikar@rediffmail.com; Tel.: 91-731-253-1906; Fax: 91-731-276-3618.

Source: Bioorg. Med. Chem. 2005, 13(6), 2109–2120.

Compounds: 223 Structurally diverse organic compounds.

Computational methods:

MLR (Multivariate Linear Regression analysis).

Data calculated:

logP (logarithm of the partition coefficient in 1-octanol/water);

$^1\chi$ (first order molecular connectivity index);

W (Wiener index defined as half-sum of the off-diagonal elements of the distance matrix of a graph);

Sz (Szeged topological index);

J (Balaban's topological J index);

χ_{eq} (equalized electronegativity);

Q (quality factor calculated as the ratio of R/s).

Chemical descriptors:

Ip_1, Ip_2, Ip_3 (indicator variables = 1 if halogens are present in the compound; benzene ring is present in the compound; hydroxyl group is present in the compound, respectively).

Results: Lipophilicity of a diverse set of organic compounds has been modeled using MLTR and distance-based topological indices. Dominating role of equalized electronegativity (χ_{eq}) has been observed. The use of indicator parameters significantly contributed to the statistical quality of the equations (Eqs. 1, 2).

$$\log P = 0.3672(\pm 0.0594)\ ^1\chi + 1.4262(\pm 0.2380)\ Ip_2 - 1.3032(\pm 0.2354)\ Ip_3 + 0.4467 \quad (1)$$
$$n = 223\ r = 0.7740\ s = 1.2187\ F = 109.1\ Q = 0.6351$$

$$\log P = 0.3172(\pm 0.5292)\ ^1\chi - 0.0027(\pm 0.0019)\ W - 0.3989(\pm 0.1840)\ J + 0.0020(\pm 6.3368 \times 10^{-4})\ Sz - 2.2060(\pm 0.4784)\ \chi_{eq} + 1.0781(\pm 0.1625)\ Ip_1 + 1.1993(\pm 0.2255)\ Ip_2 - 1.3446(\pm 0.1815)\ Ip_3 + 4.8429 \quad (2)$$
$$n = 210\ r = 0.8686\ s = 0.9202\ F = 77.2\ Q = 0.9439$$

Fig. 1 shows the plot of the calculated versus observed logP values calculated using Eq. 2.

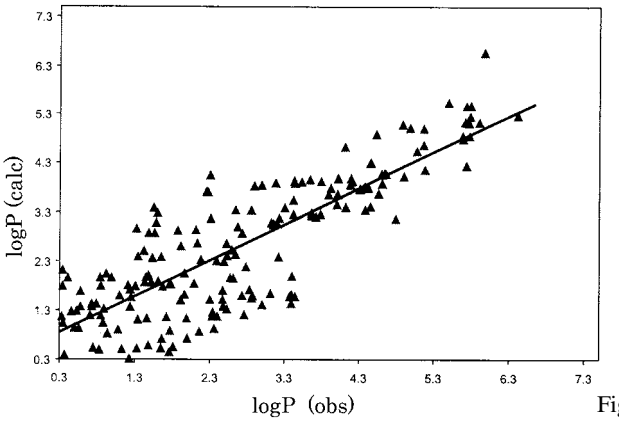

Fig. 1

The results were discussed critically on the basis various statistical parameters involved.
(B. B.)

Pharmacology

93/2005

Title: Toward a pharmacophore for kinase frequent hitters.

Authors: Aronov*, A. M.; Murcko, M. A.
Vertex Pharmaceuticals Inc.
Cambridge, MA 02139-4242, USA.
E-mail: alex_aronov@vrtx.com; Tel.: 1-617-444-6804; Fax: 1-617-444-6566.

Source: J. Med. Chem. 2004, 47(23), 5616 – 5619.

Compounds:

a) 43 Promiscuous (frequent hitter) PK inhibitors showing $K_i < 2\mu M$ against all five targets, e.g., compounds of type I and type II;
b) 209 Selective PK inhibitors.

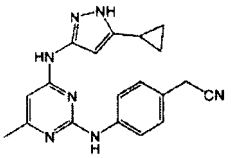

I

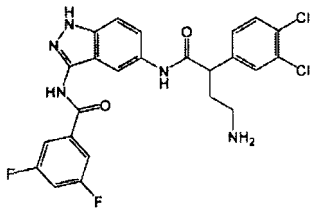

II

Biological material: Five protein kinases (PKs): protein kinase A (PKA), Src, Cdk2, Erk2, and Gsk3, of which PKA is a member of the AGC family of serine-threonine kinases, Src belongs to the tyrosine kinase superfamily, and the remaining three kinases represent various evolutionary branches of the CMGC family of serine-threonine kinases.

Data taken from the literature:

Crystal structure [atomic coordinates of PKA were taken from the Brookhaven Protein Data Bank (pdb code: 1STC)].
Crystal structure (atomic coordinates of four promiscuous ligands structure were determined by X-ray diffraction techniques).

Computational methods:

Molecular modeling (3D coordinates for the molecules in the datasets were generated with CORINA, multiconformer databases were then prepared for pharmacophore query searching using OMEGA, up to 1000 conformers/molecule were allowed, the energy window was set to 20 kcal/mol, and rmsd cutoff of 1 Å was applied to ensure adequate and diverse conformational representation).

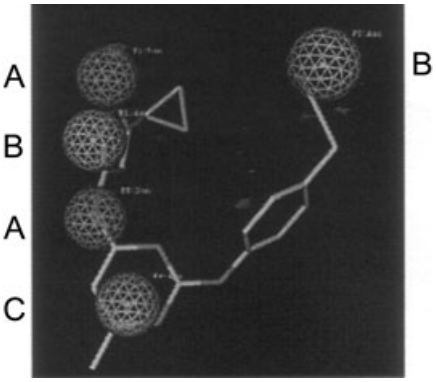

Fig. 1

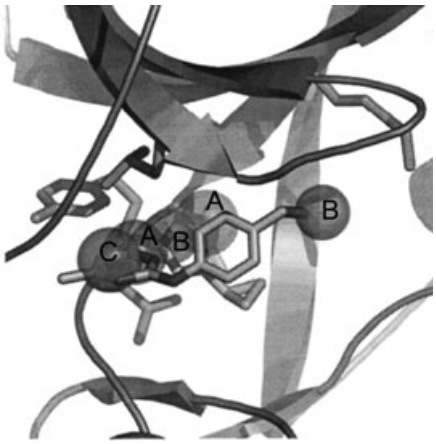

Fig. 2

Results: Small molecule PK inhibitors are widely employed as biological reagents and as leads in the design of drugs for a variety of diseases. One of the hardest challenges in kinase inhibitor design is achieving target selectivity. The following five kinases were chosen to represent the kinase space: PKA, Src, Cdk2, Erk2, and Gsk3. By utilizing X-ray structural information for four promiscuous inhibitors, a five-point pharmacophore has been proposed for kinase frequent hitters, that was able to discriminate between frequent hitters and selective ligands. Fig. 1 shows the developed pharmacophore for kinase frequent hitters, where (A), (B), and (C) denote H-bond donor, H-bond acceptor, and aromatic pharmacophoric features.

Key structural elements within the ATP site of PKA responsible for interaction with the features of the frequent hit-

ter pharmacophore are: Leu[49], Lys[72], Glu[121], Tyr[122], and Val[123]. Fig. 2 shows the kinase frequent hitter pharmacophore placed in the ATP binding site of PKA.

The crystal structure of PKA is shown in ribbon representation. The ATP binding site was aligned with other kinase structures using heavy atoms of residues 116-123 in the hinge region. A portion of the C-terminus was deleted for illustrative clarity. Key structural elements within the kinase ATP binding site responsible for interaction with the features of the frequent hitter pharmacophore are shown as capped sticks colored orange. It is expected that the ability to predict in silico the ligand's propensity for being a frequent hitter will enable medicinal chemists to make more informed decisions in the context of cross-kinase selectivity.
(B. B.)

94/2005

Title: QSAR study for a novel series of ortho monosubstituted phenoxy analogues of α_1-adrenoceptor antagonist WB4101.

Authors: Fumagalli, L.; Bolchi, C.; Colleoni, S.; Gobbi, M.; Moroni, B.; Pallavicini, M.; Pedretti, A.; Villa, L.; Vistoli G.; Valoti*, E.

Istituto di Chimica Farmaceutica e Tossicologica, Universitá di Milano

viale Abruzzi 42, I-20131 Milano, Italy.

E-mail: ermanno.valoti@unimi.it; Tel.: 39-2-5031-7553; Fax: 39-2-5031-7565.

Source: Bioorg. Med. Chem. 2005, 13(7), 2547 – 2559.

Compounds:

a) α_{1a} antagonist WB4101 of type I;
b) 16 Both (S)- and (R)-enantiomers of the analogues of WB4101 of type II, where R = H, Me, Et, t-Bu, CN, CF_3, COMe, F, Cl, SMe, SOMe, SO_2Me, NO_2, NHCOMe, NH_2, OMe;
c) [^{3}H]-8-OH-DPAT, [^{3}H]Prazosin.

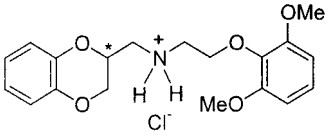

I

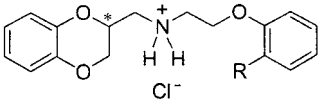

II

Biological material: α_{1a}-AR, α_{1b}-AR, α_{1d}-AR, and the 5-HT_{1A} receptors.

Data determined:

K_i [Michaelis inhibition constant (M) of both the (S)- and (R)-enantiomers of compounds required for 50% displacement of the labeled substrate assessed at the AR-subtypes and 5-HT_{1A} serotoninergic receptor in in vitro binding studies].

Computational methods:

MLR (Multivariate Linear Regression analysis).

Data calculated:

q^2 (cross-validated correlation coefficient).

Chemical descriptors:

V (fragmental volume of the aromatic substituents);
F, R (Swain-Lupton's electronic parameters, characterizing the field and resonance effects, respectively;
L [STERIMOL steric length parameter (Å)];
HBβ (the ability of accepting H bonds was parametrized by the HBβ value derived from the fragmental system Systahl v2.0).

Results: QSAR study has been performed for a novel set of 16 ortho-monosubstituted phenoxy analogues of α_1-adrenoceptor antagonist WB4101 using pK_i binding affinity data measured on the α_{1a}-AR, α_{1b}-AR, α_{1d}-AR, and the 5-HT_{1A} receptors. Comparison of the affinity values of these compounds with those of the enantiomers of the 2,6-dimethoxyphenoxy analogue, an antagonist WB4101, showed that the unsubstituted derivative (S)-1 and the o-methyl, the o-t-butyl, the o-fluoro and the o-methoxy derivatives, (S)-2, (S)-4, (S)-8 and (S)-16, respectively, display a significantly specific 5-HT_{1A} affinity, very close to (S)-WB4101 (a nanomolar antagonist). A classical QSAR (Hansch) analysis was performed using the compounds (S)-1 – (S)-16 and (S)-WB4101 to rationalize the experimental binding data (Eqs. 1 – 3).

$$pK_i(\alpha_{1a}) = 0.94(\pm 0.22)\ HB\beta - 1.51(\pm 0.28)\ R - 0.024(\pm 0.007)\ V + 7.52(\pm 0.19) \quad (1)$$
$$n = 17\ r = 0.883\ s = 0.34\ F = 15.5\ q^2 = 0.74$$

$$pK_i(\alpha_{1b}) = 0.37(\pm 0.11)\ HB\beta - 1.03(\pm 0.18)\ R - 0.0079(\pm 0.0073)\ V + 7.08(\pm 0.21) \quad (2)$$
$$n = 17\ r = 0.728\ s = 0.36\ F = 4.96\ q^2 = 0.45$$

$$pK_i(\alpha_{1d}) = -0.17(\pm 0.06)\ R + 0.87(\pm 0.19)\ L - 0.054(\pm 0.012)\ V + 4.22(\pm 0.27) \quad (3)$$
$$n = 17\ r = 0.843\ s = 0.41\ F = 11.07\ q^2 = 0.68$$

$$pK_i(5\text{-}HT_{1A}) = 0.79(\pm 0.13)\ HB\beta - 0.58(\pm 0.11)\ L - 2.15(\pm 0.16)\ R + 10.79(\pm 0.54) \quad (4)$$
$$n = 17\ r = 0.922\ s = 0.27\ F = 24.3\ q^2 = 0.81$$

The results of the study present QSAR study using the (S)-WB4101 S analogues carrying different ortho (mono)substituents at the phenoxy residue indicated that the site interacting with this moiety is subjected to tight steric constraints in both the α and 5-HT_{1A} receptors. In fact, the steric descriptors in all the equations have generally great weight and, except L in Eq. 4, their regression coefficient is always negative. The present results confirmed the putative importance of the 2,6-disubstitution, regarding in particular the two methoxy groups at the phenyl residue of 2-[(2-phenoxyethyl)aminomethyl]-1,4-benzodioxane for the interaction with the α-ARs and, especially, with the α_{1a}-AR subtype. It was also resolved that such a feature is not essential to the interaction with the 5-HT_{1A} receptor as proven by the high and specific 5-HT_{1A} affinity of the unsubstituted derivative (S)-1 as well as of several WB4101 analogues suitably ortho monosubstituted at the phenyl ring.
(B. B.)

95/2005

Title: Design, synthesis, antibacterial and QSAR studies of benzimidazole and imidazole chloroaryloxyalkyl derivatives.

Authors: Khalafi-Nezhad*, Ali; Rad, M. N. S.; Mohabatkar, H.; Asrari, Z.; Hemmateenejad, B.

Department of Chemistry, Faculty of Science, Shiraz University

Shiraz 71454, Iran.
E-mail: ali_khalafinezhad@yahoo.com; Tel./Fax: 98-711-228-0926.

Source: Bioorg. Med. Chem. 2005, 13(6), 1931 – 1938.

Compounds:

a) 5 Compounds of type I, where R^1 = H, Cl; R^2 = Cl; n = 2, 4, 5;
b) 12 Compounds of type II, where R^1 = H, Et, Me; R^2 = H, NO_2; R^3 = H, Cl; R^4 = Cl.

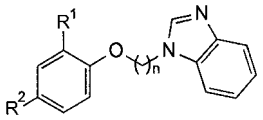

I

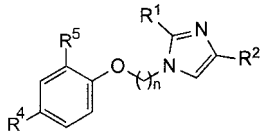

II

Biological material: 2 Bacterial species: Salmonella typhi O-901 (Gram negative) and Staphylococcus aureus A 15091 (Gram positive).

Data determined:

MIC [minimum inhibitory concentration (μg/mL) of the test substance against S. typhi and S. aureus].

Computational methods:

Molecular modeling (molecular modeling was performed using HyperChem v7 software package, geometry optimization of the molecules was carried out using the semiempirical AM1 method);

MLR (stepwise Multivariate Linear Regression analysis).

Data calculated:

Descriptors [three types of molecular descriptors were calculated using Hyperchem v7 software: HOMO and LUMO energies, dipole moments (DM), electronegativity (χ), electrophilicity (ω), softness (S), and hardness (η) were used to account the electronic features of the molecules; molecular surface area (MSA), molar volume (MV), molar refractivity (MR),lipophilicity (logP), and hydration energy (HE) were the physicochemical properties that calculated for each molecule; Dragon software was used for the calculation of topological indices such as total structure connectivity index (Xt), average connectivity index (X1A), average valence connectivity index (X2Av), sum of topological distance between N and Cl atoms (TN-Cl), and path/walk-3 randic shape index (PW3), and functional group indices including number of total primary carbons (nCp), and number of total secondary carbons (nCs)];

MEP [Molecular Electrostatic Potential (kcal/mol) was calculated using the semiempirical AM1 method].

Chemical descriptors:

nCp (number of total primary carbons).

Results: Design, synthesis, antibacterial and QSAR studies of benzimidazole of type I and imidazole chloroaryloxyalkyl derivatives of type II was performed. Some of these compounds showed considerable bactericidal activities against S. aureus and S. typhi. Calculation and mapping of MEP over the compounds revealed that negative electrostatic potentials around oxygen of the phenoxy and nitrogen of the imidazole moieties have direct effect on the antibacterial activity towards S. aureus A 15091. Fig. 1 shows the overlaid 3D structure of the imidazole and benzimidazole derivatives.

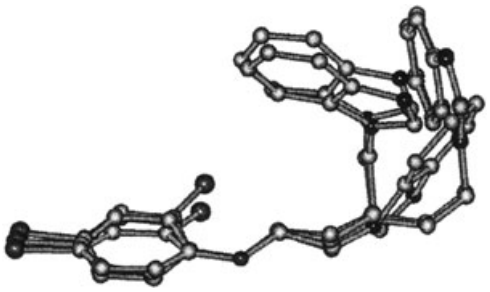

Fig. 1

Significant linear regression equations were calculated for the logMIC values against S. aureus using HOMO energy, hydration energy and number of primary carbon atoms of the molecules (Eq. 1, Eq. 2).

$$\log MIC = 1.70(\pm 0.17)\ HOMO + 0.06(\pm 0.01)\ HE + 16.77(\pm 1.50) \quad (1)$$
$$n = 13\ r = 0.979\ s = 0.062\ F = 113.5$$

$$\log MIC = 1.73(\pm 0.14)\ HOMO + 0.07(\pm 0.01)\ HE - 0.11(\pm 0.04)\ nCp + 17.37(\pm 1.1.22) \quad (2)$$
$$n = 13\ r = 0.988\ s = 0.048\ F = 121.3$$

(B. B.)

96/2005

Title: Quantitative structure-activity relationship of sesquiterpene lactones as inhibitors of the transcription factor NF-κB.

Authors: Siedle, B.; García-Piñeres, A. J.; Murillo, R.; Schulte-Mönting, J.; Castro, V.; Rüngeler, P.; Klaas, C. A.; Da Costa, F. B.; Kisiel, W.; Merfort*, Irmgard.

Institut für Pharmazeutische Wissenschaften, Lehrstuhl für Pharmazeutische Biologie, Universität Freiburg
D-79104 Freiburg, Germany.
E-mail: irmgard.merfort@pharmazie.uni-freiburg.de; Tel.: 49-761-203-8373; Fax: 49-761-203-8383.

Source: J. Med. Chem. 2004, 47(24), 6042 – 6054.

Compounds: 103 Sesquiterpene lactones (SLs) comprising 6 structural families: 44 germacranolides, 16 heliangolides, 22 guaianolides, 9 pseudoguaianolides, 2 hypocretenolides, 10 eudesmanolides, active compounds from the medicinal plant of the Asteraceae family, e.g., a germacranolide of type I and a hypocretenolide of type II.

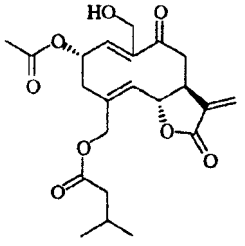

I

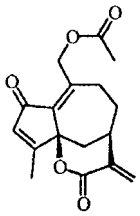

II

Biological material:

NF-κB (central transcription factor promoting the expression of over 150 target genes in response to inflammatory stimulators).

Data taken from the literature:

IC_{100} [concentration of the test substance (μM) required for total (100%) blocking of the DNA binding of NF-κB].

Computational methods:

Molecular modeling (the 3D structures of the molecules were built using the molecular modeling package HyperchemPro v6.02, energy minimizations were performed with the MM+ force field using the Polak-Ribiere minimization algorithm, low energy conformations of the SLs were created using the conformational search option, the final geometries were obtained with the semiempirical AM1 method;

MLR (Multiple Linear Regression analysis was performed using the SAS v6.12 statistical software package, relevant descriptors were selected using the REG procedure).

Data calculated:

Descriptors (constitutional, topological, electrostatic and quantum chemical descriptors were calculated using the software CAChe: total number of α,β unsaturated carbonyl structures in the molecule, UNC; α-methylene-γ-lactone, ML; conjugated ester groups, UNA; conjugated keto or aldehyde functions, ENONE; number of oxygen atoms, ATOM; number of hydroxyl groups, OH; octanol water partition coefficient, LOGP; electron affinity, EA; dipole moment, DIPOL; molar refractivity, MR; connectivity indices, CN0 – 2; shape indices, SH1 – 3; highest occupied molecular orbital, HOMO; lowest unoccupied molecular orbitals, LUMO1 – 3).

Results: The sesquiterpene lactones (SLs) inhibit the transcription factor NF-κB probably by alkylating cys[38] in the DNA binding domain of the p65 subunit. The SLs have been suggested to serve as lead compounds for the design of new antiinflammatory drugs. In this study, QSAR analysis of a set of 103 different SLs as inhibitors of NF-κB has been performed using MLR. Sub-groups of SLs were subjected to analysis. The results indicated that topological and structure-coding parameters explained the NF-κB inhibitory activity of SLs possessing a rigid skeleton (furanoheliangolides and guaianolides), whereas in the case of flexible skeletons (germacranolides, such as germacrolides and melampolides),inhibition might be mostly determined by reactivity parameters, such as the number and type of α,β-unsaturated carbonyl structural elements. The following significant linear regression equations were calculated for all major skeletal classes (Eq. 1), for germacranolides (Eqs. 2,3), heliangolides (Eq. 4).

$$pIC_{100} = 0.239(\pm 0.054)\ UNC + 0.431(\pm 0.164)\ ML + 0.648(\pm 0.143)\ EA + 0.050(\pm 0.023) \quad (1)$$
$$n = 103\ r = 0.772\ s = 0.381\ F = 36.2$$

$$pIC_{100} = 0.271(\pm 0.068)\ UNC + 0.452(\pm 0.226)\ ML + 0.518(\pm 0.163)\ EA - 2.597(\pm 0.224) \quad (2)$$
$$n = 60\ r = 0.779\ s = 0.329\ F = 28.8$$

$$pIC_{100} = 1.012(\pm 0.206)\ ML + 0.347(\pm 0.071)\ UNA + 0.933(\pm 0.134)\ EA - 2.893(\pm 0.210) \quad (3)$$
$$n = 37\ r = 0.904\ s = 0.201\ F = 49.1$$

$$pIC_{100} = 1.060(\pm 0.141)\ ENONE + 0.731(\pm 0.126)\ SH2 - 0.628(\pm 0.132)\ ATOM - 3.462(\pm 1.101) \quad (4)$$
$$n = 16\ r = 0.933\ s = 0.233\ F = 26.8$$

For the rest of the chemical types the following linear regression equations were calculated (chemical type, n , r, s, F, descriptors): guaianolides, 22, 0.818, 0.282, 8.58, UNC, CN2, MR, OH; eudesmanolides, 10, 0.860, 0.145, 5.70, SH1, SH2, ATOM. Fig. 1 shows the plot of the calculated versus experimental pIC_{100} values for heliangolides computed using Eq. 4.

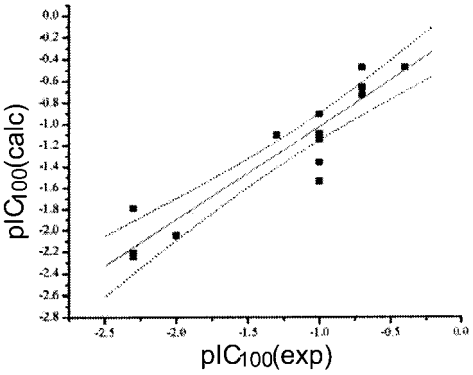

Fig. 1

The QSAR studies described here and in previous studies showed that inhibtory activity conditions correlated mostly with the structure-cytotoxcity requirements. Therefore, it was unlikely to separate the desired therapeutic effects from the unwanted side effects such as cytotoxicity. This is also valid for the allergenic properties of the compounds. In order to avoid this problem the SLs could be either applied externally, or they could be designed as a prodrug that would be liberated at the location of inflammation for the treatment of chronic inflammatory diseases.

(B. B.)

97/2005

Title: Anti-inflammatory activity and QSAR studies of compounds isolated from Hyacinthaceae species and Tachiadenus longiflorus Griseb. (Gentianaceae)

Authors: du Toit, K.; Elgorashi, E. E.; Malan, S. F.; Drewes, S. E.; van Staden, J.; Crouch, N. R.; Mulholland*, D. A.

Natural Products Research Group, School of Chemistry, University of KwaZulu-Natal

Durban 4041, South Africa.

E-mail: mulholld@ukzn.ac.za; Tel.: 27-31-260-1108; Fax: 27-31-260-3091.

Source: Bioorg. Med. Chem. 2005, 13(7), 2561 – 2568.

Compounds: 22 Homoisoflavanones and structurally related compounds, e.g., 11 compounds of type I, where $R^1 = H$,

MeO; R^2 = H, OH, OMe; R^3 = H, OH, OMe; R^4 = OH, OMe; R^5 = OH, OMe; R^6 = H, OH, OMe.

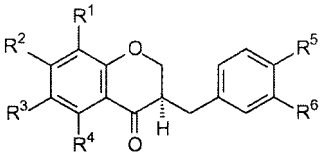

I

Biological material:

a) Southern African Hyacinthaceae species, and the Madagascan gentian Tachiadenus longiflorus Griseb;
b) Purified human recombinant cyclooxygenase (COX-2) enzyme and COX-1 enzyme obtained from sheep seminal vesicles.

Data determined:

AIA [specific inhibition (%) of isolated COX-1 and COX-2 enzymes];

I% [inhibition of prostaglandin synthesis in microsomal cell preparations (%)].

Computational methods:

Molecular modeling: modeling and structural optimization were performed using PC Spartan Pro v1.0 modeling software, MM+ and AM1 minimized models were used for molecular and electronic calculations, ground state energies were optimized using MMFF94 force field, the rigid and planar structure of type I with $R^1 = R^2 = R^3 = R^4 = R^5$ = OH, R^6 = H (Ia) was used as reference and manipulation of this structure rendered the consequent structures, molecular dynamics (MD) simulations were used to sample conformational space before minimization using the MM+ force field, the obtained minimum energy structures were used as starting point for semi-empirical minimization using the AM1 method];

MLR (stepwise Multivariate Linear Regression analysis performed using the STATISTICA software package).

Data calculated:

Descriptors: [the following physicochemical descriptors were used to characterize the structures of the homoiso-flavanones and structurally related compounds using the ACD, Insight II and the PC Spartan Pro v1.0 programs: strain energy, heat of formation, volume, surface area, aqueous phase energy, dipole moment, enthalpy, entropy;, molar refractivity, MR (Å^3); parachor, P (Å^3); density, refractive index, RI; surface tension, ST (dyn/cm); polarizability, POL (Å^3); logarithm of the partition coefficient in 1-octanol/water, logP, Van der Waals interaction energy, VE (kcal/mol); Coulombic interaction energy, CE (kcal/mol); and nonbonded interaction energy NIE (kcal/mol); volume of a space filling model, SV; surface area, SA; aqueous phase energy, ES; dipole moment, DP; vibrational enthalpy, VEL; and vibrational entropy, TE; electron potential at atomic level, EP, e.g., at C-4 or O-1 according to Fig. 1].

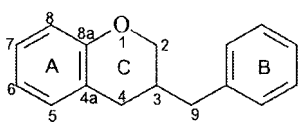

Fig. 1

Results: A QSAR investigation has been performed to study the antiinflammatory activities of 22 structurally related homoisoflavanones and structurally related compounds isolated from Hyacinthaceae species and Tachiadenus longiflorus Griseb and four synthetic compounds. Six homoisoflavanone and structurally related compounds showed significantly high levels of anti-inflammatory activity in the microsomal fraction assay (I%). Only one compound exhibited a high level of anti-inflammatory activity in the COX-1 enzyme assay and no significant activity was detected in the COX-2 enzyme assay. The biological screening results were used as independent variables in the QSAR study. The physicochemical descriptors calculated were used to characterize the structures of the compounds. Stepwise MLR yielded three significant linear regression equations (Eqs. 1, 3).

$$AIA = -1.094\ MR + 18.930\ D - 131.212\ C\text{-}4 + 0.018\ EF + 4.935\ VE\ \text{-}138.688 \quad (1)$$
$$n = 22\ r = 0.8173\ s\ \text{not given}\ F\ \text{not given}$$

$$AIA = -1.126\ MR + 21.241\ D - 135.740\ C\text{-}4 + 0.146\ ES + 5.011\ VE - 142.126 \quad (2)$$
$$n = 22\ r = 0.8165\ s\ \text{not given}\ F\ \text{not given}$$

$$AIA = 30.730\ C\text{-}5 - 122.678\ C\text{-}4 - 0.076\ MV + 0.031\ EF + 3.206\ VE - 72.274 \quad (3)$$
$$n = 22\ r = 0.8165\ s\ \text{not given}\ F\ \text{not given}$$

The regression models demonstrated the importance of properties describing volume, density and steric bulk, thus indicating restricted entrance to the binding site. The energy terms, heat of formation and aqueous phase energy could be associated with the importance of the conformation of the chemical structures. Polarizability and the formation of dipoles represented by the Van der Waals interaction energy and molar refractivity also played a major role in ligand-receptor binding. Different parameters that, in turn, are influenced by a variety of factors played a role in the activity of the compounds studied and one parameter may be counterbalanced by another. It was suggested that the derived models provided valuable parameter guidelines for those properties influencing the anti-inflammatory activity of the studied compounds.
(B. B.)

Toxicology and Environmental Science

98/2005

Title: QSAR by LFER model of cytotoxicity data of anti-HIV 5-phenyl-1-phenylamino-1 H-imidazole derivatives using principal component factor analysis and genetic function approximation.

Authors: Roy*, Kunal; Leonard, J. T.

Drug Theoretics and Cheminformatics Laboratory, Division of Medicinal and Pharmaceutical Chemistry, Department of Pharmaceutical Technology, Jadavpur University

Kolkata 700 032, India.

E-mail: kunalroy_in@yahoo.com; Tel.: 91-33-2414-6676; Fax: 91-33-2414-6677.

Source: Bioorg. Med. Chem. 2005, 13(8), 2967 – 2973.

Compounds: 42 Compounds of type I, where $R^1 = CH_3$, $CH(CH_3)_2$; $R^2 = H$, SH; $R^3 = H$, F, Cl, Br, NO_2, CH_3, OCH_3, CH_2CH_3, SCH_3; $R^4 = H$, Br, Cl, OCH_3, CN, $OCOCH_3$, COOH, $CONH_2$.

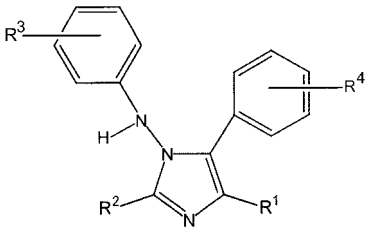

I

Biological material: MT4 cells.

Data taken from the literature:

CC_{50} [concentration of the test substance (μM) required for 50% reduction of MT4 cell viability].

Computational methods:

MLR (Multivariate Linear Regression analysis);

FA (Factor Analysis followed by Varimax rotation);

GFA (Genetic Function Approximation for the generation of multiple QSAR models by evolving random initial models using a genetic algorithm);

LOO (Leave-One-Out cross-validation).

Data calculated:

Descriptors [$B4_{m\_A}/B1_{m\_A}/L_{m\_A}/MR_{m\_A}$: $B_4/B_1/L/MR$ value of meta substituent (R^3) present on the phenyl ring of 1-phenylamino fragment; σ_{p_A}: Hammett σ constant of para substituent (R^3) present on the phenyl ring of 1-phenylamino fragment; π_{m_B}: π value of meta substituent (R^4) present on 5-phenyl ring of the imidazole nucleus];

SDEP (Standard Deviation Error in Prediction);

PRESS (sum of the squared deviation between the predicted and measured binding affinities for every molecule);

r^2_{bsr} (bootstrap r^2);

q^2 (cross-validated correlation coefficient).

Chemical descriptors:

σ (Hammett's constant characterizing the electron withdrawing power of the substituent);

π (Hansch-Fujita's substituent constant characterizing hydrophobicity);

STERIMOL [L, B_1, B_2, B_3, B_4 steric parameters (Å)]

MR (molar refractivity);

Indicator variables [I_{R1_CH3}: indicator variable 1 if methyl group is present at the 4 position of the imidazole nucleus; I_{R2_SH}: indicator variable 1 if thiol group is present at the 2 position of the imidazole nucleus; $I_{m\_B\_Hydrogen\_Donor}$: indicator variable 1 if any hydrogen donor substituent is present at the meta position of the 5-phenyl nucleus; $I_{23\_A\_NIL}$: indicator variable 1 if no substituent is present at 2 and 3 positions of the N-phenylamino fragment].

Results: QSAR analysis of the CC_{50} cytotoxicity data of 42 compounds of type I was performed using FA-MLR and GFA methodologies. FA was used as data-preprocessing step to identify the important predictor variables contributing to the response variable and to avoid collinearities. The MLR equations were statistically validated using the LOO algorithm. GFA was also used on the same data set to develop QSAR equations, which produced the same best equation as obtained with FA-MLR. FA of the data matrix consisting of cytotoxicity data, physicochemical parameters and indicator variables revealed that 12 factors could explain 96.1% of variance of the data matrix. Based on the results of FA, Eq. 1 was derived with six variables.

$$pCC_{50} = 0.143(\pm 0.138)\ B4_{m\_A} - 1.722(\pm 1.108)\ \sigma_{p\_A} + 0.257(\pm 0.124)\ \pi_{m\_B} - 0.302(\pm 0.104)\ I_{R2\_SH} - 0.512(\pm 0.177)\ I_{m\_B\_Hydrogen\_Donor} - 0.375(\pm 0.181)\ I_{23\_A\_NIL} + 1.193(\pm 0.400) \quad (1)$$
$$n = 42\ r = 0.907\ s = 0.152\ F_{6,35} = 27.1\ q^2 = 0.737$$

$$SDEP = 0.187\ S_{PRESS} = 0.210\ r^2_{bsr} = 0.824$$

The best equation obtained in a stepwise fashion was Eq. 2.

$$pCC_{50} = 0.278(\pm 0.223)\ MR_{m\_A} - 1.685(\pm 1.080)\ \sigma_{p\_A} + 0.252(\pm 0.122)\ \pi_{m\_B} - 0.300(\pm 0.099)\ I_{R2\_SH} - 0.515(\pm 0.173)\ I_{m\_B\_Hydrogen\_Donor} - 0.366(\pm 0.175)\ I_{23\_A\_NIL} + 1.404(\pm 0.177) \quad (2)$$
$$n = 42\ r = 0.912\ s = 0.148\ F_{6,35} = 28.7\ q^2 = 0.740$$

$$SDEP = 0.168\ S_{PRESS} = 1.183\ r^2_{bsr} = 0.832$$

Analysis of the regression models suggested that a thiol substituent at 2 position of the imidazole nucleus decreases the cytotoxicity relative to the unsubstituted congener. Presence of hydrogen bond donor group at meta position of the phenyl ring present at 5 position of the imidazole nucleus also reduces cytotoxicity. Absence of any substituent at 2 and 3 positions of the phenyl ring of 1-phenylamino fragment reduced the cytotoxicity. The negative coefficient of r indicates that presence of electron-withdrawing substituents at the para position of the phenyl ring of the 1-phenylamino fragment is not favorable for the cytotoxicity. Lipophilicity of meta substituents of the 5-phenyl ring increases cytotoxicity. The coefficients of molar refractivity (MR_m) and STERIMOL parameters for meta substituents (L_m, $B1_m$ and $B4_m$) of the phenyl ring of 1-phenylamino fragment indicate that the length, width and overall size of meta substituents are relevant factors for the cytotoxicity.

(B. B.)

99/2005

Title: Acute toxicity of benzoic acids to the crustacean Daphnia magna.

Authors: Kamaya*, Y.; Fukaya, Y.; Suzuki, K.

Department of Environmental Science for Human Life, Faculty of Agriculture, Shizuoka University

836 Ohya, Shizuoka 422-8529, Japan.

E-mail: ahykama@agr.shizuoka.ac.jp; Fax: 81-54-237-3028.

Source: Chemosphere 2005, 59(2), 255–261.

Compounds: 22 Benzoic acid derivatives: benzoic acid, BA; 4-methoxybenzoic, 4-M; 3,4-dimethoxybenzoic, 3,4-DM; 3,4,5-trimethoxybenzoic acid, 3,4,5-TM; 2-hydroxybenzoic, 2-H; 3-hydroxybenzoic acid, 3-H; 4-hydroxybenzoic acid, 4-H; methyl 4-hydroxybenzoate, M; 4-hydroxy-3-methoxybenzoic, VA; 3-hydroxy-4-methoxybenzoic, i-VA; 4-hydroxy-3,5-dimethoxybenzoic, SA; 4-hydroxybenzyl alcohol, HB; 4-hydroxybenzaldehyde, HBA; 2,3-dihydroxybenzoic acid, 2,3-DH; 2,4-dihydroxybenzoic, 2,4-DH; 2,5-dihydroxybenzoic, 2,5-DH;

2,6-dihydroxybenzoic, 2,6-DH; 3,4-dihydroxybenzoic, 3,4-DH; 3,5-dihydroxybenzoic, 3,5-DH; 2,3,4-trihydroxybenzoic acid, 2,3,4-TH; 2,4,6-trihydroxybenzoic acid, 2,4,6-TH; 3,4,5-trihydroxybenzoic, 3,4,5-TH.

Biological material: Daphnia magna, a freshwater crustacean test species often used for ecotoxicological evaluation of industrial chemicals.

Data taken from the literature:

logP (logarithm of the partition coefficient in 1-octanol/water).

Data determined:

EC_{50} [effective concentration of the test substance (mmol/L, mg/L) required for 50% acute immobilization of the daphnids in 24 h and 48 h experiment under neutralized condition (initial pH: 7.45 ± 0.05)].

Computational methods:

MLR (Multivariate Linear Regression analysis was calculated using JMP 5.0 J software of the SAS Institute).

Data calculated:

logP [logarithm of the partition coefficient in 1-octanol/water was calculated using the online version of the CLOGP program (Daylight Chemical Information Systems Web site)].

Chemical descriptors:

N_{OH} (number of hydroxyl groups);

MW [molecular weight (g/mol)].

Results: QSAR analysis of the acute immobilization toxicity of 22 benzoic acid derivatives to D. magna has been performed using MLR involving logP and N_{OH} descriptors. Toxicity, expressed as EC_{50} value, depended primarily on the number and position of phenolic hydroxyl groups. The benzoic acids with ortho-substituted hydroxyl groups were more toxic than benzoic acids with meta- and/or para-substituted hydroxyl groups. In contrast, methoxy substitution exerted relatively small and variable effects on the toxicity. Of the tested compounds, the 2,4,6-TH showed the highest toxicity in the 48 h EC_{50} of 10μmol/L. 2,4,6-TH was 700 times as toxic as the parent benzoic acid (48 h $EC_{50} = 7.0$ mmol/L) and about two orders of magnitude higher than those previously reported for monohalogenated benzoic acid derivatives against D. magna. Within the subgroups based on the number of hydroxyl groups (N_{OH}), the toxicity variations due to the position of hydroxyl groups correlated with the logarithms of logP. The toxicity of benzoic acids could be expressed using simple linear and parabolic regression equations (Eqs. 1, 2).

$$\log(EC_{50}) = -0.869\ \log P - 0.321\ N_{OH}^2 - 0.494 \quad (1)$$
$$n = 19\ r = 0.959\ s = 0.270\ F = 104$$

$$\log(EC_{50}) = -1.13\ \log P - 1.55\ N_{OH} + 1.63 \quad (2)$$
$$n = 12\ r = 0.974\ s = 0.229\ F = 103$$

(B. B.)

ADME

100/2005

Title: In silico ADME modelling. Prediction models for blood-brain barrier permeation using a systematic variable selection method.

Authors: Narayanan*, R.; Gunturi, S. B.

Bioinformatics Division, Advanced Technology Center, Tata Consultancy Services, 1, Software Units Layout

Madhapur, Hyderabad 500 081, India.

E-mail: narayananr@atc.tcs.co.in; Tel.: 91-40-5567-3581; Fax: 91-40-5567-2222.

Source: Bioorg. Med. Chem. 2005, 13(8), 3017 – 3028.

Compounds:

a) 116 Drugs and drug-like compounds;
b) 91 Known Drugs and drug-like compounds.

Data taken from the literature:

logBB (in vivo blood-brain permeation data of the compound).

Computational methods:

VSMP [variable Selection and Modeling method based on the Prediction All subset regression (ASR) is one of the variable selection procedures that can select the best descriptor subset from the given dataset, but is computationally intensive, we have introduced two controllable parameters, namely, the inter-correlation coefficient between pairs of independent descriptors (r_{int}) and cross-validation correlation coefficient (Q^2) into ASR, to accelerate the speed of computation, the inter-correlation coefficient was set between descriptors as 0.75];

MLR (Multivariate Linear Regression analysis);

LOO (Leave-One-Out cross-validation).

Data calculated:

Descriptors (a total of 324 descriptors were calculated using the QSAR module of the in-house software, 'Biosuite' of which 7 are physicochemical descriptors, 7 are geometrical descriptors, 11 are structural descriptors and the remaining 299 are topological descriptors, e.g., atomic type E-state index, SsssN; atomic level based AI topological descriptor, AIssssC; Kappa shape index of order 1, κ^1; topological Xu index; autocorrelation descriptor (Moran) weighted by atomic Van der Waals radius-order 3; 2D Van der Waals surface area];

AlogP98 (logarithm of the partition coefficient in 1-octanol/water calculated using the AlogP algorithm).

Results: Quantitative structure-property relationship (QSPR) models have been built based on in vivo logBB data of 88 diverse compounds, 324 descriptors and employing a systematic variable selection method, VSMP. The best three-parameter model developed using VSMP, contained the SsssN, AlogP98, and Van der Waals surface area as descriptors ($r = 0.8425$, $q^2 = 0.6788$, $F = 68.5$ and $SE = 0.4165$); the best four-parameter model contained the κ^1, SsssN, AIssssC, and AlogP98 ($r = 0.8638$, $q = 0.7177$, $F = 60.7$ and $SE = 0.3919$). Fig. 1 shows the plot of the cross-validated logBB versus experimental logBB values calculated using the best four parameter linear regression model.

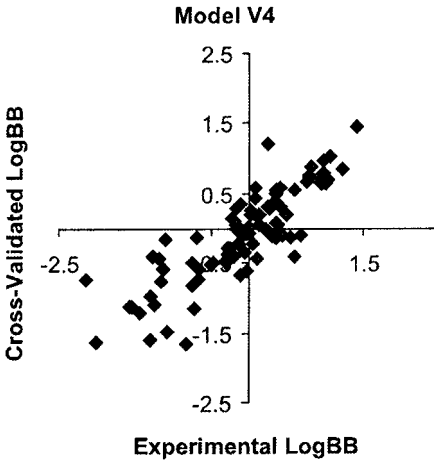

Fig. 1

The performance of the models was validated using three test sets taken from the literature, and the results were compared with the results from other reported computational approaches. The Test_set_III included 91 compounds from the literature with known qualitative BBB indication and was used for virtual screening studies. The success rate of the reported models was 82% for the BBB+ compounds and a similar success rate was observed for BBB-compounds. The models possessed excellent predictive power and proposed to be used for virtual screening, where selection and prioritization of candidates is required.
(B. B.)

101/2005

Title: Validation of model of cytochrome P4502D6. An in silico tool for predicting metabolism and inhibition.

Authors: Kemp, C. A.; Flanagan, J. U.; van Eldik, A. J.; Maréchal, J.-D.; Wolf, C. R.; Roberts, G. C. K.; Paine, M. J. I.; Sutcliffe*, M. J.

Departments of Biochemistry and Chemistry, University of Leicester

University Road, Leicester, LE17RH, England.

E-mail: sjm@le.ac.uk; Tel.: 44-116-252-3601; Fax: 44-116-252-3369.

Source: J. Med. Chem. 2004, 47(22), 5340–5346.

Compounds:

a) Spirosulfonamide, an atypical (no basic nitrogen) cytochrome P4502D6 substrate;
b) 33 Compounds from the NCI, e.q., type NCI-17383.

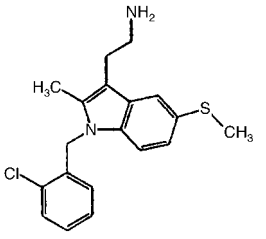

I

Biological material: Cytochrome P4502D6.

Data taken from the literature:

Compounds [111 druglike compounds, within the same molecular weight range as the known Cytochrome P4502D6 inhibitors <600), were retrieved from the National Cancer Institute (NCI) database].

Data determined:

IC_{50} [concentration of the test substance (μM) required for 50% inhibition of cytochrome P4502D6 using a fluorescence based screening approach].

Computational methods:

Molecular modeling (the homology model of CYP2D6 was built as described previously using the comparative modeling program Modeler with five structural templates: P450s cam, terp, eryF, BM3, and 2C5, docking studies were carried out using the program GOLD v2.0 with the ChemScore fitness function, the docking was performed with a standard GA protocol and an active site cavity defined as a sphere with a 20 Å radius centered on the heme Fe atom, 10 solutions for of each ligand were generated and ranked using the ChemScore fitness function, only the best ranked solution of each ligand was included in further analysis, inspection of the results was performed using the molecular visualization package InsightII);

GOLD [flexible protein-ligand docking program featuring a (i) genetic algorithm methodology for protein docking; (ii) full ligand and partial protein flexibility; (iii) energy functions partly based on conformation and non-bonded contact information from the Cambridge Structural Database (CSD)].

GA (Genetic Algorithm).

Results: Modeling of cytochrome P4502D6 is a particularly important target because this enzyme is involved in the oxidation of at least 50 drugs. Previously the authors have described the combined use of homology modeling and molecular docking in order to correctly position a range of substrates in the CYP2D6 active site with the known sites of metabolism above the heme. In this study, validation of the model of cytochrome P4502D6 has been performed that can be used as an in silico tool for predicting metabolism and inhibition. The proposed docking approach identified correctly the site of metabolism of the atypical cytochrome P4502D6 substrate, spirosulfonamide. The same method was employed to screen a small compound database of 33 compounds from the NCI database by docking it into the developed cytochrome P4502D6 homology model using the program GOLD v2.0. Experimental IC_{50} values for the 33 compounds were measured. The docked scored correlated with experimental IC_{50} values with a regression coefficient of $r^2 = 0.61$ ($q^2 = 0.59$). Fig. 1 shows the plot of the experimental log(IC_{50}) values versus ChemScore values (kJ/mol) for each NCI compound for the best ranked docked solution.

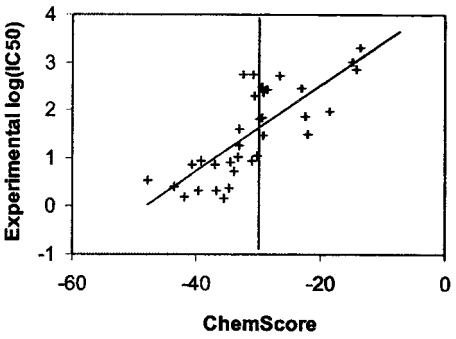

Fig. 1

Fig. 2 shows the docked structure of compound NCI_17383 in the CYP2D6 homology model. The heme moiety and key protein residues are also shown (dark structures).

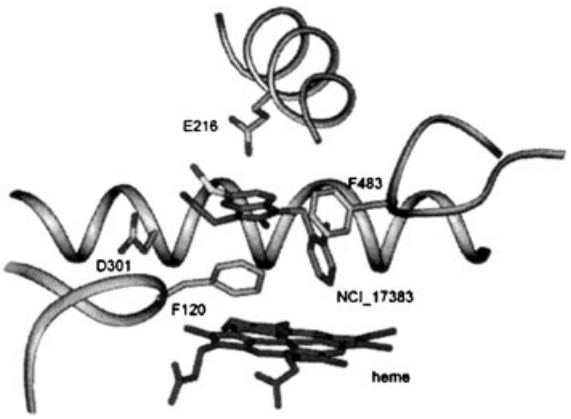

Fig. 2

The method was able to discriminate between tight and weak binding compounds and correctly identified several novel inhibitors. It was suggested that the combination of homology modeling and molecular docking is a useful in silico tool for predicting cytochrome P4502D6 inhibition. The method is best used as a filter in a multifilter database screen. (B. B.)

3D QSAR

102/2005

Title: 3D-QSAR CoMFA studies on trypsin-like serine protease inhibitors. A comparative selectivity analysis.

Authors: Bhongade, B. A.; Gouripur, V. V.; Gadad*, A. K.
Department of Medicinal Chemistry, College of Pharmacy, J. N. Medical College
Belgaum 590 010, Karnataka, India.
E-mail: akgadad@rediffmail.com; Tel.: 91-831-247-1399/1-868-662-147; Fax: 91-831-247-2387.

Source: Bioorg. Med. Chem. 2005, 13(18), 2773–2782.

Compounds: 39 Compounds of type I, where R^1 = H, F, Cl, OMe, OH, Me; R^2 = H, Cl; R^3 = H, OH, F, Cl, Br, Me, OMe, NO_2, NEt_2, Ph, 3,4-naphthyl; X = N, CH, NMe, Y = NH, N, O.

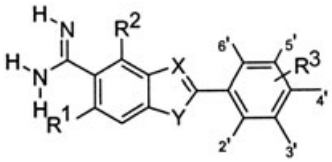

I

Biological material: Trypsin-like serine proteases: uPA, tPA, factor Xa, thrombin, plasmin, and trypsin.

Data taken from the literature:

K_i [Michaelis inhibition constant (μM) representing the affinity of the substrate to the serine proteases uPA, tPA, factor Xa, thrombin, plasmin, and trypsin].

Computational methods:

ComFA [Comparative Molecular Field Analysis of the molecules was carried out represented by their steric and electrostatic fields sampled at the intersections of a three-dimensional lattice (2 Å grid increment) using an sp^3 carbon atom probe with a charge of +1, ClogP was used as an additional descriptor, molecular superimposition was carried out on the template structure using atom-based RMS fit method, all regression analyses were done using PLS algorithms in SYBYL v6.7];

PLS (Partial Least Squares projections to latent structures analysis);

LOO (Leave-One-Out cross-validation).

Data calculated:

ClogP (logarithm of the partition coefficient in 1-octanol/water was calculated using ChemDraw Ultra v6.0 software integrated with CambridgeSoft Software Development Kit);

rmsd [root mean square deviation (Å) of the position of the corresponding atoms of two superimposed molecular structures];

SEP (Standard Error of Prediction);

SEE (Standard Error of Estimation);

q^2 (cross-validated correlation coefficient).

Results: The inhibitory activities of a series of indole/benzimidazole-5-carboxamidines of type I have been tested against trypsin-like serine proteases. CoMFA models were generated for the training set of the compounds in order to study their selectivity toward various trypsin-like serine proteases. The CoMFA models were established from the training set of 25–29 molecules and validated by predicting the activities of 7–8 test set molecules (protease, N_{opt}, r^2, r^2_{cv}, F, SEE, SEP, steric, electrostatic contributions): tPA, 7, 0.987, 0.584, 224.8, 0.140, 0.809, 57.2, 42.8; fXa, 2, 0.811, 0.513, 47.3, 0.497, 0.798, 56.1, 43.9; thrombin, 3, 0.845, 0.504, 39.9, 54.5, 45.5; plasmin, 2, 0.822, 0.629, 57.8, 0.404, 0.583, 61.8, 38.2; trypsin, 2, 0.838, 0.583, 59.5, 0.348, 0.558, 58.2, 41.8. Introduction of ClogP as an additional descriptor slightly deteriorated the statistical quality and predictive performance of the CoMFA models. The validated CoMFA models were used to generate 3D steric and electrostatic fields contour maps, providing guidance toward possible modification of molecules for better selectivity and activity. Fig. 1 shows the CoMFA steric and electrostatic STDDEV*COEFF contour plots for trypsin inhibition (A polyhedron: sterically favored, B polyhedron: sterically disfavored, C polyhedron: negatively charge favored, D polyhedron: positively charge favored).

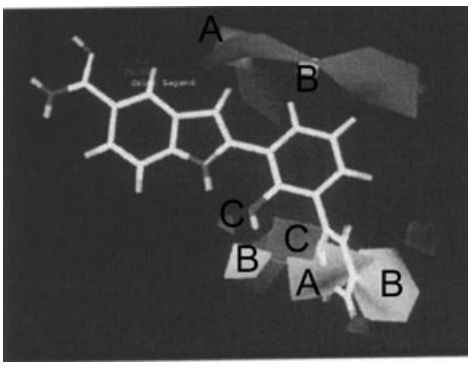

Fig. 1

The present 3D-QSAR studies reveals the selectivity trends of indole/benzimidazole-5-carboxamidines, which may be useful for designing novel selective serine protease inhibitors of therapeutic interest. In all the cases, the sterically fa-

vorable green contours were in the vicinity of C-3 substitution and embedded in the 3′-phenyl ring, whereas in tPA they were observed next to the 3′-phenyl ring. The sterically disfavored yellow contours were observed in the vicinity of 3′-phenyl ring of the compounds. The electrostatic contour plots displayed red polyhedron amid the 2′-OH and 3′-phenyl ring suggesting that increase in activity may be anticipated by moderate electronegative substitutions at 3 – -position of 2-phenyl ring, while moderate electropositive substituents at C-3, 2′, 6'-positions may enhance the tPA, fXa, plasmin and thrombin activity as shown by the presence of positively charge favored blue contours. It was corroborated that the nature of the substituent at C-6 position is the crucial factor in determining the selectivity trends of various serine protease inhibitors. It was found, that optimum low electron density substituent at C-6 may enhance the tPA and fXa activity as is indicated by the presence of the blue contour near 6-H of compound. Replacement of C-6 proton with a halogen (chloro) markedly decreased the tPA, fXa and thrombin inhibition, whereas no significant change was observed in case of plasmin and trypsin (compound 28). It was suggested that the CoMFA models developed for the trypsin-like serine protease inhibitors of type I may be useful in the rational design of selective serine protease inhibitors against cancer as well as anticoagulant or antithrombotic chemotherapeutics.
(B. B.)

103/2005

Title: The substrate specificity of SARS coronavirus 3C-like proteinase.

Authors: Fan, K.; Ma, L.; Han, X.; Liang, H.; Wei, P.; Liu, Y.; Lai*, LuHua.

State Key Laboratory of Structural Chemistry of Stable and Unstable Species, College of Chemistry, Peking University

Beijing 100871, China.

E-mail: lhlai@pku.edu.cn; Fax: 86-10-6275-1725.

Source: Biochem. Biophys. Res. Commun. 2005, 329(3), 934 – 940.

Compounds: 34 Peptide substrates.

Biological material: 3C-like proteinase of severe acute respiratory syndrome coronavirus (SARS).

Data taken from the literature:

Crystal structure [atomic coordinates of the 3C-like proteinase of SARS were taken from the Brookhaven Protein Data Bank (pdb code: 1UK4)].

Data determined:

k_{cat}/K_m [enzymatic cleavage activities of the mutated substrate peptides ($mM^{-1}min_{-1}$) were measure using a HPLC based peptide cleavage assay, where the concentration of the SARS 3C-like proteinase is 5.41μM or 27.05μM for the substrates].

Computational methods:

ComFA [Comparative Molecular Field Analysis of the molecules was carried out represented by their steric and electrostatic fields sampled at the intersections of a three-dimensional lattice (2 Å grid increment) using an sp^3 carbon atom probe with a charge of +1, all regression analyses were done using PLS algorithms in SYBYL v6.91];

PLS (Partial Least Squares projections to latent structures analysis);

LOO (Leave-One-Out cross-validation).

Data calculated:

q^2 (cross-validated correlation coefficient).

Results: The 3C-like proteinase of SARS is a key target for structure based drug design against SARS. In this study the substrate specificity of SARS coronavirus 3C-like proteinase has been investigated using the hydrolysis activities of 34 designed peptide substrates. The conserved core sequence of the native cleavage site was optimized for high hydrolysis activity. Residues at position P4, P3, and P3′ are known to be critical for substrate recognition and binding, and enhancement of the β-sheet conformation tendency is also helpful. In addition, it was found that a salt bridge between position P3 and Glu^{166} of the enzyme enhances the activity of the substrate. Using the enzymatic cleavage activity data a significant CoMFA model was derived ($q^2 = 0.661$, $r^2 = 0.822$, $s = 0.429$, $F_{2,20} = 46.2$, steric and electrostatic contribution = 81.8% and 18.2%, respectively). Fig. 1 shows the superimposed 22 substrate structures and the contour plot of the CoMFA model indicating that increasing positive charge at position P3 is favored (A), and large hydrophobic residue at position P2 is favored (B) or unfavored (C), which is compatible with the crystal structure.

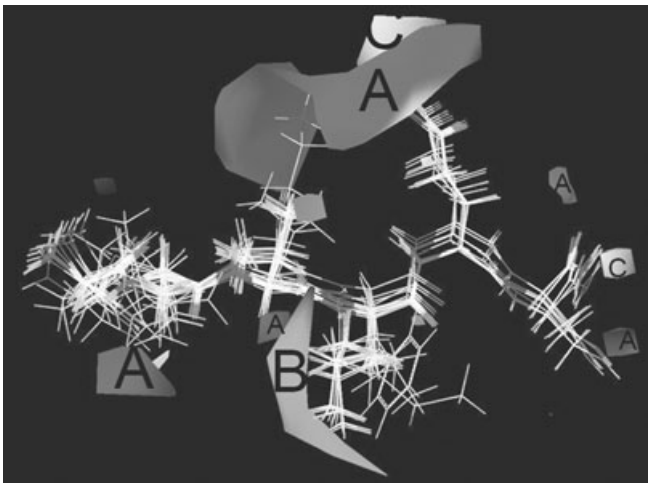

Fig. 1

Based on the mutation data and the predictive CoMFA model, a multiply mutated octapeptide S24 was designed for higher enzymatic cleavage activity. The hydrolysis activity of S24 was measured and found to be the highest among all designed substrates. The measured activity value (0.634 mM^{-1} min^{-1}) was close to that predicted by CoMFA (0.58 mM^{-1} min^{-1}). It was concluded that the developed model might be helpful for the research of the mechanism of substrate recognition of coronavirus 3C-like proteinase.
(B. B.)

104/2005

Title: Comparative molecular similarity indices analysis (CoMSIA) studies of 1,2-naphthoquinone derivatives as PTP1B inhibitors.

Authors: Sobhia*, M. E.; Bharatam, P. V.

Department of Medicinal Chemistry, National Institute of Pharmaceutical Education and Research (NIPER)

Sector-67, S. A. S. Nagar (Mohali) 160062, India.

E-mail: mesophia@niper.ac.in

Source: Bioorg. Med. Chem. 2005, 13(6), 2331 – 2338.

Compounds: 34 Compounds of type I, where $R^1 - R^5$ = diverse substituents.

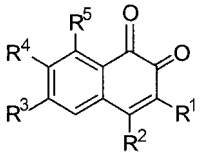

I

Biological material: Recombinant human protein tyrosine phosphatase-1B (PTP1B).

Data taken from the literature:

IC_{50} [concentration of the test substance (dimension not given) required for 50% in vitro inhibition of recombinant human PTP1B using fluorescein diphosphate].

Computational methods:

Molecular modeling (molecular modelling studies were carried out using SYBYL v6.8, implemented on an SGI Octane2 workstation, the most active molecule of the series was subjected to simulated annealing, the lowest energy conformer was selected and minimized using Tripos force field parameters and the Powell method, all the other molecules were built from the template molecule, partial atomic charges were calculated using Gasteiger-Hückel charges);

CoMSIA [Comparative Molecular Similarity Indices Analysis of the molecules was carried out as an alternative approach to CoMFA based on similarity indices calculated at the intersections of a three dimensional lattice, the five physicochemical properties for CoMSIA (steric, electrostatic, hydro-phobic, and hydrogen bond donor and acceptor) were evaluated using a common probe atom with 1 Å radius, +1.0 charge, and hydrophobicity and hydrogen bond property values of +1, the value of an attenuation factor α was 0.3 for the Gaussian-type distance dependence];

PLS (Partial Least Squares projections to latent structures analysis);

LOO (Leave-One-Out cross-validation).

Data calculated:

logP (logarithm of the partition coefficient in 1-octanol/water was estimated using HyperCHem v6.0);

SEE (Standard Error of Estimation);

r^2_{cv} (cross-validated correlation coefficient).

Chemical descriptors:

MW [molecular weight (g/mol)];

NRB (number of rotable bonds);

HBD, HBA (number of hydrogen bond donor and acceptor centres, respectively).

Results: In this study a CoMSIA analysis of nonpeptidic 1,2-naphthoquinone as derivatives of type I as potential PTP1B inhibitors was performed. The compound set was subjected to property filters and segregated into training and test set. The most active molecule was subjected to simulated annealing dynamics method and the lowest energy conformer was minimized again and considered as the bioactive conformation. Database-inertial alignment using the selected template molecule was utilized for aligning the molecules. Several CoMSIA analyses were performed to obtain the best model. The statistical parameters of the best CoMSIA model were the following: n = 25 training set an 9 test set molecules, $r^2_{cv} = 0.454$, $N_{opt} = 5$, SEE = 0.066, F = 245.9, steric fields: steric = 0.112, electrostatic = 0.279, hydrophobic = 0.297, H-bond donor = 0.089, H-bond acceptor = 0.223. The most active molecule was type I with $R^1 = (CH_2)_2CO_2Et$, R^2 = indole, $R^3 = R^4 = R^5 = H$ (Ia). Fig. 1 shows the CoMSIA contour map of the H-bond acceptor field contributions around Ia, where A and B areas represent H-bond acceptor favored and disfavored areas, respectively.

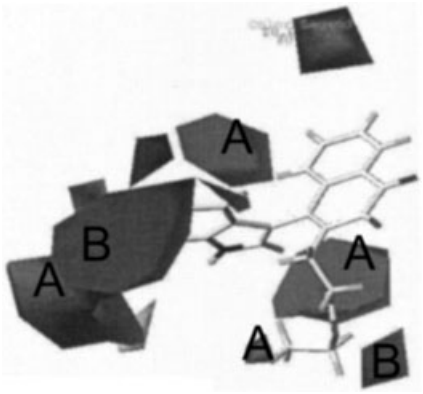

Fig. 1

As the crystal structure of PTP1B-naphthoquinone derivative is not known, the hydrogen bond donor and acceptor fields of this CoMSIA study indicate the probable H-bond sites on the enzyme for explaining the interaction between this class of compounds and the protein.
(B. B.)

105/2005

Title: Novel 5-HT_7 receptor inverse agonists. Synthesis and molecular modeling of arylpiperazine- and 1,2,3,4-tetrahydroisoquinoline-based arylsulfonamides.

Authors: Vermeulen*, E. S.; van Smeden, M.; Schmidt, A. W.; Sprouse, J. S.; Wikström, H. V.; Grol, C. J.

Department of Medicinal Chemistry, Center for Pharmacy, State University of Groningen

A. Deusinglaan 1, NL-9713 AV Groningen, The Netherlands.

E-mail: e.s.vermeulen@farm.rug.nl; Tel: 31-50-311-8007; Fax: 31-50-360-0390.

Source: J. Med. Chem. 2004, 47(22), 5451 – 5466.

Compounds:

a) Twenty-two structurally diverse 5-HT7 receptor inverse agonists, e.g., 3 compounds of type I, where Ar = 3-CH_3-C_6H_5 (Ia), 3-OH-C_6H_5 (ib), 1-naphthyl (1c);
b) [^{3}H]-5C, ^{33}P cAMP, ^{33}PATP.

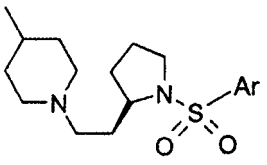

I

Biological material:

a) Cloned rat 5-HT7 serotonin receptors expressed in HEK-293 cells;
b) Adenylate cyclase.

Data taken from the literature:

Sequence [sequence of 449 amino acids of the human 5-HT7A receptor was taken from the SwissProt database (entry P34969)].

Data determined:

K_i [Michaelis inhibition constant (nM) representing the affinity of the substrate to displace [^{3}H]-5CT at the 5-HT7 receptor];

EC_{50} [effective concentration of the test substance (nM) required for 50% adenylate cyclase agonist activity].

Computational methods:

Molecular modeling [all molecular computations were performed on a Silicon Graphics workstations, conformational analyses, molecular structures were sketched in their protonated, positively charged state from standard fragments in MacroModel, conformational analyses were performed using the Monte Carlo Multiple Minimum (MCMM) search protocol, minimizations were performed using the Truncated Newton Conjugate Gradient (TNCG) minimization method within the MM2 force field, employing a distance dependent water continuum as implemented in MacroModel, pharmacophore identification was done using the RMSFIT module of APOLLO, homology modeling of the receptor was performed on the basis of the sequence of 449 amino acids of the human 5-HT7A receptor and the evolutionary highly conserved amino acids within the rhodopsin-based family of G-protein-coupled receptors followed by energy minimization of the ensemble of the 7 transmembrane helices of the model, ligands were manually docked into the binding site, the merged complex of ligand and receptor was minimized with the Tripos force field, Gasteiger-Hückel charges and the conjugate gradient method yielding properly docked ligands];

ComFA [Comparative Molecular Field Analysis of the molecules was carried out represented by their steric and electrostatic fields sampled at the intersections of a three-dimensional lattice (2 Å grid increment) using an sp^3 carbon atom probe with a charge of +1, all regression analyses were done using PLS algorithms in SYBYL v6.8];

PLS (Partial Least Squares projections to latent structures analysis);

LOO (Leave-One-Out cross-validation).

Data calculated:

logP (logarithm of the partition coefficient in 1 octanol/water was calculated using Pallas v1.2);

pK_a (negative logarithm of the acidic dissociation constant was calculated using Pallas v1.2);

rmsd [root mean square deviation (Å) of the position of the corresponding atoms of two superimposed molecular structures];

q^2 (cross-validated correlation coefficient).

Results: 3D QSAR analysis of a set of novel 5-HT7 receptor inverse agonists of type I was performed in order to study interactions with the constitutive active 5-HT7 receptor. All ligands produced a decrease of adenylate cyclase activity, indicative of their inverse agonism. 3D QSAR analyses of a set of 22 inverse agonists yielded a pharmacophore model and a CoMFA model ($R^2 = 0.97$, $q^2 = 0.64$, SE = 0.18). The correlation coefficient between predicted and experimental pK_i values was 0.987. Fig. 1 shows the developed pharmacophore model for 5-HT7 inverse agonism and 5-HT7 receptor agonism.

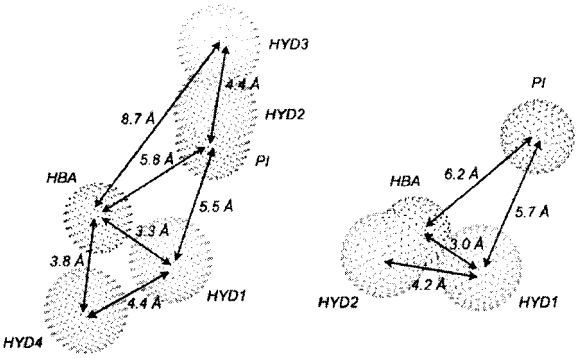

Fig. 1

The pharmacophore model shows similarities with recently published pharmacophore models for 5-HT7 receptor agonism and antagonism. Docking of inverse agonists at the binding site of a model of the helical parts of the 5-HT7 receptor revealed interesting molecular interactions and a possible explanation for observed structure-activity relationships. Fig. 2 shows the close-up of molecular interactions between Ib and the binding site of the 5-HT7 receptor, where nonessential hydrogen atoms have been omitted.

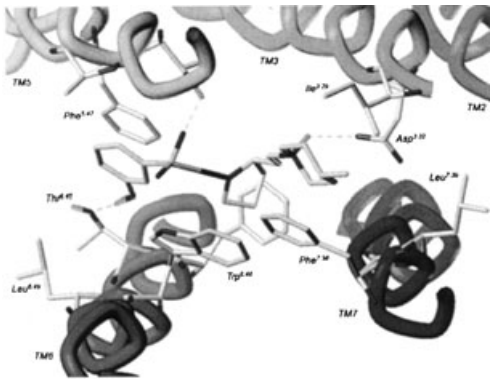

Fig. 2

In case of the 5-HT7 receptor, it was indicated that agonists and inverse agonists occupy the same binding site, but additional pharmacophoric features induce different conformational changes of the receptor resulting in activation by agonists and deactivation by inverse agonists.
(B. B.)

106/2005

Title: CoMFA study of piperidine analogues of cocaine at the dopamine transporter. Exploring the binding mode of the 3α-substituent of the piperidine ring using pharmacophore-based flexible alignment.

Authors: Yuan, H.; Kozikowski, A. P.; Petukhov*, P. A.

Department of Medicinal Chemistry and Pharmacognosy, College of Pharmacy, University of Illinois at Chicago

833 S. Wood Street, Room 539, Chicago, IL 60612, USA.

E-mail: pap4@uic.edu; Tel: 1-312-996-4174; Fax: 1-312-996-7107.

Source: J. Med. Chem. 2004, 47(25), 6137 – 6143.

Compounds:

a) 21 Compounds of type I, where R = diverse substituents;
b) 9 Compounds of type I, where R = diverse substituents, where R = CO_2H, $CO_2CH_2CH_3$, $CO_2(CH_2)_3Ph$, $CONHCH_3$, CONHAd, $CONHCH_2C_6H_5$, $CON(CH_3)_2$, $CONCH_3Bn$, type IV moiety;
c) 8 Compounds of type I, where R = CO_2H, CO_2CH_3, $(CH_2)_2$-trans-CH = CH-CO_2CH_3, CONHPh, CONHAd, CH_3, CH_2OH, CH_2F;
d) [^{3}H]DA.

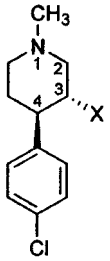

I

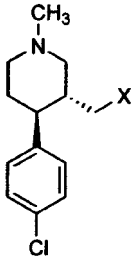

II

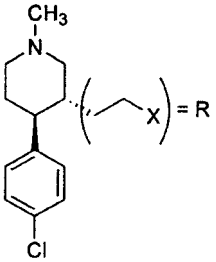

III

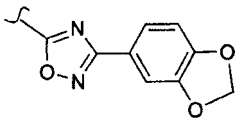

IV

Biological material: Dopamine transporter (DAT).

Data taken from the literature:

Datasets [structural and biological data (K_i) were collected from the papers previously published by Kozikowski et al. and Petukhov et al.];

K_i [Michaelis inhibition constant (nM) representing the affinity of the substrate to displace [^{3}H]DA at the rat nerve endings (synaptosomes) obtained from rain regions enriched in DAT receptor].

Computational methods:

Molecular modeling [all molecular modeling and CoMFA studies were performed on an SGI or a Linux computer using the Sybyl v6.9 software, all compounds were assigned into three series C1, C2, and C3 according to the number of carbon atoms between the attachment point of the 3R-substituent and its first polar atom, the molecules were built and minimized using the Tripos force field and Gasteriger-Marsili charges, a protonated piperidine nitrogen was adopted for all ligands used in this study, pharmacophore searching was accomplished using the GASP, once a pharmacophore was generated, the 3D structure of one of the three representative molecules, compound of type II with R = IV (IIa) was used as a template in structure alignment for all molecules of the three series using FlexS, a top-ranked conformer for each compound was initially utilized in CoMFA modeling, the MOPAC charges for FlexS and CoMFA modeling were calculated using the AM1 method];

ComFA [Comparative Molecular Field Analysis of the molecules was carried out represented by their steric and electrostatic fields sampled at the intersections of a three-dimensional lattice (2 Å grid increment) using an sp^3 carbon atom probe with a charge of +1, all regression analyses were done using PLS algorithms in SYBYL v6.9];

GASP (genetic algorithm for flexible molecular overlay, the fitness of an alignment is characterized by a combination of three criteria: the number and similarity of overlaid features, the volume overlap of the alignment, and the internal van der Waals energy of the molecular conformations).

FLEXS [automatic method for the reproduction of experimentally determined structures of ligand bound structures by structurally superimposing pairs of ligands for approximating their putative binding site geometry, one of the ligands is treated as flexible (test ligand) and is placed onto the other ligand which is treated as a rigid structure (reference ligand)];

LOO (Leave-One-Out cross-validation);

PLS (Partial Least Squares projections to latent structures analysis);

LOO (Leave-One-Out cross-validation).

Data calculated:

q^2 (cross-validated correlation coefficient).

Results: A 3D-QSAR CoMFA study of piperidine-based analogues of cocaine with flexible 3R-substituents has been performed in order to explore the binding mode of the 3α-substituent of the piperidine ring using pharmacophore-based flexible alignment. A set of three different GASP pharmacophore models were generated based on three representative sets of compounds of types I – III. The flexible superposition of all studied compounds was performed for each pharmacophore model using the FlexS algorithm, all sets of the overlaid structures with the top-ranked conformers were used for CoMFA modeling. Compared with the initial models, the conventional correlation coefficients r^2 for the optimized models 1 and 2 were improved from 0.90 and 0.837 to 0.997 and 0.993, respectively. The LOO coefficients q^2 for the optimized models 1 and 2 were improved from 0.515 and 0.296 to 0.828 and 0.849, respectively. The results of the two CoMFA models suggest that both steric and electrostatic interactions play important roles in the binding of the 3R-substituents of the piperidine-based analogues of cocaine. The contributions from steric and electrostatic molecular fields for model 1 were 0.621 and 0.379, respectively. The contributions from steric and electrostatic fields for model 2 were 0.493 and

0.507, respectively. The two highly predictive CoMFA models indicate that the 3R-substituent has two possible binding modes at the DAT. The fact that two distinct models were obtained indicates that the 3R-substituent may adopt multiple binding modes. Fig. 1 a shows the CoMFA contour maps of optimized model 1, in the electrostatic contour map, greater affinity is correlated with more positive charge near A fields and more negative charge near other contour; in the steric contour map Fig. 1 b greater affinity is correlated with more bulky groups near A contours and less bulky groups near B contour.

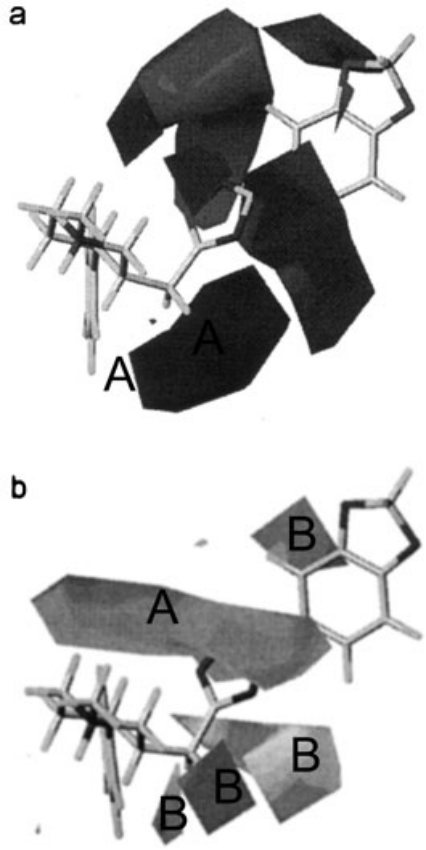

Fig. 1

The CoMFA contour maps provided a visual representation of the putative binding modes of the 3R-substituent of the piperidine-based analogues of cocaine and can be applied to design novel DAT inhibitors that may be useful for the treatment of cocaine abuse and certain neurological disorders.
(B. B.)

107/2005

Title: Comparative molecular field analysis and comparative molecular similarity indices analysis of human thymidine kinase 1 substrates.

Authors: Bandyopadhyaya, A. K.; Johnsamuel, J.; Al-Madhoun, A. S.; Eriksson, S.; Tjarks*, W.

Division of Medicinal Chemistry, College of Pharmacy, The Ohio State University

Columbus, OH 43210, USA.

E-mail: tjarks.1@osu.edu; Tel.: 1-614-292-7624; Fax: 1-614-292-2435.

Source: Bioorg. Med. Chem. 2005, 13(5), 1681 – 1689.

Compounds: 31 Compounds of type I, where R^1 = H, ET, $CH_2C{\equiv}CH$, n-Bu, CH_2Ph, $CH_2CHOHCH_2OH$, i-Pr; R^2 = H, Me, I, Br, CH = CHBR, CH_2CH_2Cl, NH_2, F; R^3 = H, OH; R^4 = H, OH; R^3 and R^4 together = -CH_2-; R^5 = H, OH, N_3, CH_2N_3, OMe, OEt, F; R^6 = H.

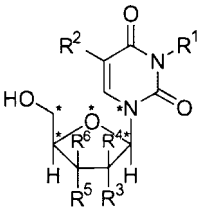

I

Biological material: Thymidine kinase 1 (TK1).

Data taken from the literature:

PR (relative TK1 phosphorylation rates of TK1 substrates).

Computational methods:

Molecular (all molecular modeling calculations were carried out on a SGI O2 workstation using SYBYL v6.9 molecular modeling software energy minimizations were carried out using the Tripos force field, the Powell method, and Gasteiger-Hückel, the atoms used for the alignments are indicated by asterisks in type I);

ComFA [Comparative Molecular Field Analysis of the molecules was carried out represented by their steric and electrostatic fields sampled at the intersections of a three-dimensional lattice (2 Å grid increment) using an sp^3 carbon atom probe with a charge of +1, all regression analyses were done using PLS algorithms in SYBYL v6.9];

CoMSIA [Comparative Molecular Similarity Indices Analysis of the molecules was carried out as an alternative approach to CoMFA based on similarity indices calculated at the intersections of a three dimensional lattice, the five physicochemical properties for CoMSIA (steric, electrostatic, hydrophobic, and hydrogen bond donor and acceptor) were evaluated using a common probe atom with 1 Å radius, +1.0 charge, and hydrophobicity and hydrogen bond property values of +1, the value of an attenuation factor α was 0.3 for the Gaussian type distance dependence];

PLS (Partial Least Squares projections to latent structures analysis);

LOO (Leave-One-Out cross-validation).

Data calculated:

q^2 (cross-validated correlation coefficient).

Results: TK1 is a critically important target for antiviral and anticancer chemotherapy. In this study, CoMFA and CoMSIA has been performed in order to analyze the phosphorylation capability of a series of 31 TK1 substrates of type I. Significant CoMFA and CoMSIA models were developed for 26 training set molecules showing the following statistical parameters (model, N_{opt}, q^2, r^2, s, F, steric, electrostatic, hydrophobic, H-bond donor, H-bond acceptor fields) CoMFA, 7, 0.651, 0.980, 0.207, 129.3, 2.14, 0.786, –, –, –; CoMSIA, 8, 0.619, 0.994, 0.104, 372.2, 0,099, 0.502, 0.399, 0.996, 0.003. The predictive capacity of both models was successfully validated by predicting the known phosphorylation rates of five TK1

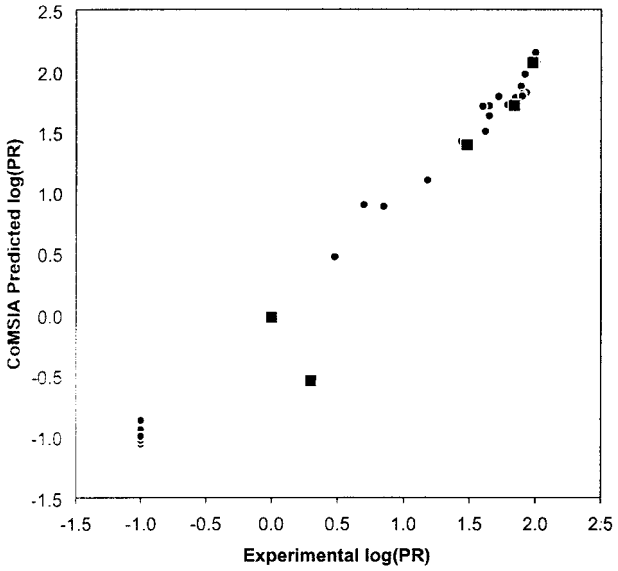

Fig. 1

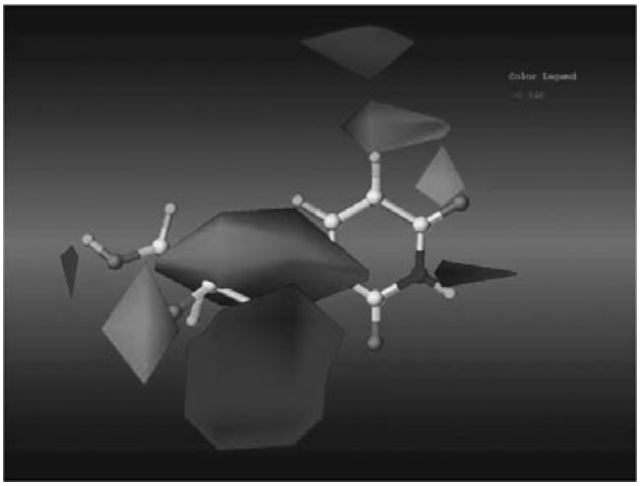

Fig. 2

substrates that were not included in the training set. Contour maps obtained from CoMFA and CoMSIA models correlated with the experimentally developed structure-activity relationships. The predictive capability of the CoMSIA model was found to be superior to that of the CoMFA model. Fig. 1 shows the plot of the predicted versus experimental logPR values of the compounds int the training set (circles) and test set (squares) calculated using the best CoMSIA model.

Fig. 2 shows the CoMSIA SD*Coeff contour plots for electrostatic fields with a substrate of type I as the reference, where lighter depict areas were positively charged groups increase activity (contour level 0.040) and dark areas indicate increase in the activity with negatively charged groups (contour level 0.040).

A combined use of both the CoMFA and the CoMSIA model appeared to be most suitable to predict the activities of novel TK1 substrates designed in silico. It was suggested that the 3D structural coordinates obtained from the CoMFA and CoMSIA contour maps could be used in database mining for existing unknown TK1 substrates.
(B. B.)

108/2005

Title: A three-dimensional in silico pharmacophore model for inhibition of Plasmodium falciparum cyclin-dependent kinases and discovery of different classes of novel Pfmrk specific inhibitors.

Authors: Bhattacharjee*, Apurba, K.; Geyer, J. A.; Woodard, C. L.; Kathcart, A. K.; Nichols, D. A.; Prigge, S. T.; Li, Z.; Mott, B. T.; Waters*, N. C.

Division of Experimental Therapeutics, Walter Reed Army Institute of Research

Silver Spring, MD 20910-7500, USA.

E-mail: apurba.bhattacharjee@na.amedd.army.mil; Tel.: 1-301-319-9043; Fax: 1-301-319-9449.

Source: J. Med. Chem. 2004, 47(22), 5418 – 5426.

Compounds:

a) 15 Structurally diverse training set compounds (CDK inhibitors), e.g., the most potent and least potent compounds of types I and II, respectively;
b) 16 Hit compounds, e.g., types III, and IV.

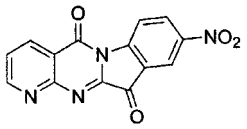

I

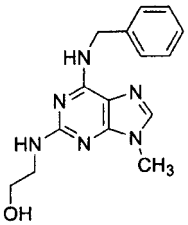

II

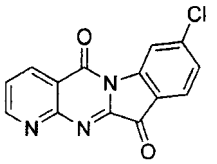

III

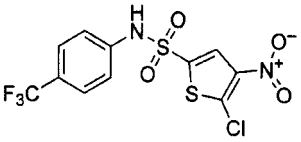

IV

Biological material: Cyclin-dependent kinases (CDKs) from Plasmodium falciparum (Pfmrk).

Data taken from the literature:

Compounds	(CIS in house multiconformer database containing over 290 000 compounds underlying the catDB software that allows conformational flexibility during the search of the database);
Crystal structure	(atomic coordinates of 50 X-ray crystal structures of CDKs with bound inhibitors were determined by X-ray diffraction techniques).

Data determined:

IC_{50}	[concentration of the test substance (μM) required for 50% inhibition of the Pfmrk];
ADME/ toxicity	[ADME/toxicity evaluations were carried out by using Cerius2 and TOPKAT methodology as implemented in catDB].

Computational methods:

Catalyst [computer program for automatic generation of pharmacophore models for a training set of molecules specifying the relative alignments and active conformations of the ligands consistent with the binding to a common receptor site, the pharmacophore model (hypothesis) consists of a collection of features necessary for the biological activity of the ligands arranged in 3D space, the common ones being hydrogen bond acceptor, hydrogen bond donor, and hydrophobic features];

TOPKAT [Toxicity Prediction by Komputer Assisted Technology, is a general purpose modular package for predicting toxicity using multivariate methods and several types of descriptors (electronic, topological shape, and substructure (3000 molecular fragments)].

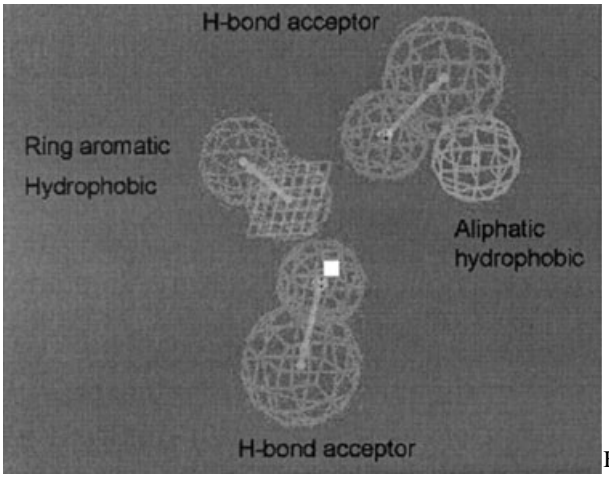

Fig. 1

Results: The cell division cycle is regulated by a family of CDKs. The plasmodial CDK is an attractive antimalarial drug target. In this study a 3D pharmacophore model has been derived for inhibitors of P. falciparum CDKs and used for the database search of novel Pfmrk specific inhibitors. A 3D QSAR Catalyst pharmacophore model has been developed for the inhibition of a P. falciparum CDK, known as Pfmrk, from a set of 15 structurally diverse kinase inhibitors displaying a wide range of activity. The pharmacophoric features includes two hydrogen bond acceptor functions and two hydrophobic sites including one aromatic-ring hydrophobic site feature (Fig. 1).

Although the model was not based on experimental X-ray structure data of the known CDK2 structure, it was consistent with what is known from nearly 50 X-ray crystal structures of CDKs with bound inhibitors. The model agreed well with the structure-functional requirements for binding of the CDK inhibitors in the ATP binding pocket. The pharmacophore model contains features shared by a wide range of general CDK inhibitors, as well as features that appear to be Pfmrk-specific. Despite the complexity of P. falciparum CDK activity, the predicted Pfmrk inhibition from the derived pharmacophore model was robust. The derived pharmacophore model was used as a template for a search of the in-house 3D multiconformer database yielding 16 potent Pfmrk inhibitors. Fig. 2 shows the mapping of one of the potent hit compounds (type III, $IC_{50} = 3.5\mu M$), onto the pharmacophore.

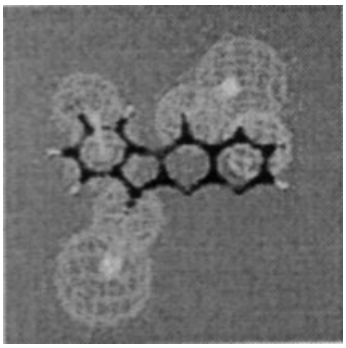
Fig. 2

The predicted inhibitory activities of some of these Pfmrk inhibitors from the molecular model agreed quite well with the experimental inhibitory values obtained in an in vitro CDK assay.

(B. B.)

109/2005

Title: Classical and three-dimensional QSAR for the inhibition of [^{3}H]ponasterone A binding by diacylhydrazine-type ecdysone agonists to insect Sf – 9 cells.

Authors: Nakagawa*, Y.; Takahashi, K.; Kishikawa, H.; Ogura, T.;

Minakuchi, C.; Miyagawa, H.

Division of Applied Life Sciences, Graduate School of Agriculture, Kyoto University

Kyoto 606-8502, Japan.

E-mail: naka@kais.kyoto-u.ac.jp; Tel.: 81-75-753-6117; Fax: 81-75-753-6123.

Source: Bioorg. Med. Chem. 2005, 13(4), 1333-1340.

Compounds:

a) 43 Diacylhydrazine congeners of type I, where R^1 and R^2 = diverse substituents;

b) 9 Diacylhydrazine congeners of type II, where R^1 = 2-Cl, 3,5-$(CH_3)_2$; R^2 = n-Pr, n-Bu, n-Pen, n-Hex, n-Hep, n-Noni-Hex, i-Pen;

c) [^{3}H]PoA ([^{3}H]Ponasterone A).

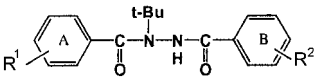

I

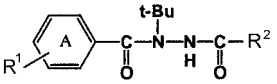

II

Biological material: Intact Sf-9 cells in cultured integument of Chilo suppressalis expressing the ecdysone receptor.

Data taken from the literature:

Crystal (atomic coordinates of the compound of type I with $R^1 = R^2 = H$ (RH-5849) were determined by X-ray diffraction techniques);

logP (logarithm of the partition coefficient in 1-octanol/water).

Data determined:

IC_{50} [concentration of the test substance (M) required for 50% inhibition of binding of [^{3}H]PoA to the ecdysone receptor expressed in Sf-9 cells].

Computational methods:

Molecular modeling (molecular structures were constructed by modifying the X-ray structure of RH-5849 pre-

viously reported, structure optimization was performed using the semiempirical PM3 method, the charges were calculated employing the AM1 method, all ligands were automatically aligned for CoMFA analysis using the Align Database command in Sybyl based on the which common skeletal chain C–C–N–N C–C of the template, the hydrophobic effect was evaluated using logP and $(logP)^2$ as lattice independent external descriptors);

QSAR (Hansch-Fujita QSAR analysis was performed using the OREG v2.05 system using logP descriptors);

ComFA [Comparative Molecular Field Analysis of the molecules was carried out represented by their steric and electrostatic fields sampled at the intersections of a three-dimensional lattice (2 Å grid increment) using an sp^3 carbon atom probe with a charge of +1, all regression analyses were done using PLS algorithms in SYBYL v6.91];

PLS (Partial Least Squares projections to latent structures analysis);

LOO (Leave-One-Out cross-validation).

Data calculated:

logP (logarithm of the partition coefficient in 1-octanol/water was calculated using MacLogP v4.0);

D_A, D_B [descriptors expressing the length of the A-ring and B-ring moieties, respectively, of the compounds of type I and II (?)];

q^2 (LOO cross-validated correlation coefficient).

Results: CoMFA analysis combined with logP values as external parameters yielded a highly significant and predictive model (Eq. 1), with steric, electrostatic and logP contributions of 35.3%, 18.4%, 24.6%, respectively.

$$pIC_{50} = 1.620\ logP - 0.197\ (logP)^2 + [CoMFA] + 2.891 \quad (1)$$
$$n = 50\ r = 0.963\ s = 0.214\ F = 92.8\ q^2 = 0.593$$

$$logP_{opt} = 4.11$$

Fig. 1 shows the plot of observed and calculated pIC_{50} values calculated using Eq. 1, where compounds represented by open circles were omitted from the analysis.

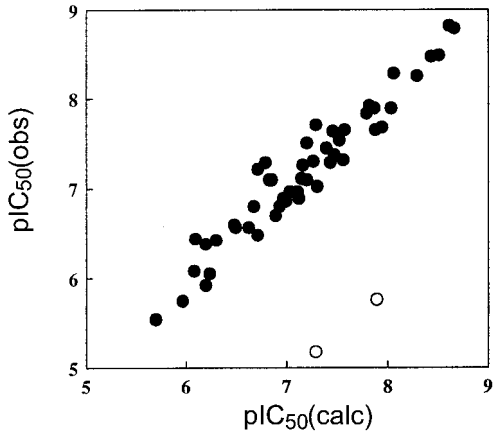

Fig. 1

Fig. 2 shows the isoenergy contour plot around chromafenozide [type I with $R^1 = 3,5\text{-}(CH_3)_2$, $R^2 = 2\text{-}CH_3\text{-}3,4\text{-}(CH_2CH_2CH_2O)$-], where A and light contours indicate regions, where steric bulk increases or decreases, respectively, binding.

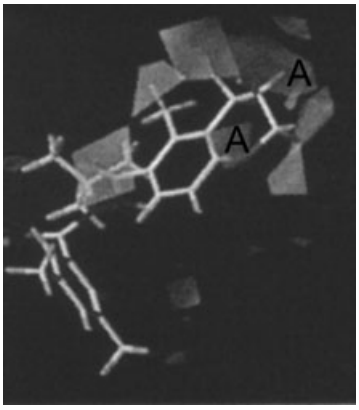

Fig. 2

Sterically favorable molecular fields were observed at the 3-and 4-positions of the benzene (B-ring) next to the t-butyl group, and a sterically unfavorable field was evidenced at the 2-position. Another sterically unfavorable field surrounding the favorable field observed at the 4-position of the B-ring. Electrostatically negative fields were observed near the C=O moiety, above the benzene ring, and at the 4-position of the B-ring. The optimum hydrophobicity of compounds in terms of logP was calculated to be 4.1. The results of the 3D SAR analyses were consistent with those obtained from the previously reported classical QSAR for 2-chlorobenzoyl analogs containing diverse para-substituents. The high activity of potent insecticides such as tebufenozide and chromafenozide could be rationalized by the derived CoMFA model. It was suggested that the CoMFA method is a useful tool in the design of novel compounds and in understanding the structural details and mechanism of the ligand-receptor interactions. (B.B.)

DataBase, Virtual Screening

110/2005

Title: Novel cyclooxygenase-1 inhibitors discovered using affinity fingerprints.

Authors: Hsu, N.; Cai, D.; Damodaran, K.; Gomez, R. F.; Keck, J. G.; Laborde, E.; Lum, R. T.; Macke, T. J.; Martin, G.; Schow, S. R.; Simon, R. J.; Villar, H. O.; Wick, M. M.; Beroza*, P.

Telik, Inc.,

3165 Porter Drive, Palo Alto, CA 94304, USA.

E-mail: pberoza@telik.com; Tel.: 1-650-845-7836; Fax: 1-650-845-7844.

Source: J. Med. Chem. 2004, 47(20), 4875–4880.

Compounds: 19 Known nonsteroidal antiinflammatory drugs (NSAIDs) from different structural classes: acemetacin, carprofen, diclofenac of type I, fenbufen, ibuprofen of type II, etodolac, diflunisal, indomethacin, indopforen, isoxicarn, ketoprofen, phenylbutazone, naproxen, piroxicam, pirprofen, nimesulide, 6-methoxynaphthalene-2-acetic acid, sulindac, tenoxicam.

Biological material: Cyclooxygenase-1 (COX-1), (prostaglandin G/H synthase).

Data determined:

IC_{50} [concentration of the test substance (μM) required for 50% inhibition of COX-1].

Computational methods:

TRAP (Target Related Affinity Profiling technology characterizes small molecules by their affinities to a panel of proteins, a compound's set of binding affinities to this panel, its affinity fingerprint, is the descriptor used to construct computational models for activity against a particular therapeutic target, the TRAP algorithms select compounds for testing on the basis of the spatial relationships among active, inactive, and untested molecules in this 12-dimensional space, affinity fingerprints are not constructed from chemical structure; thus, they are naturally suited for finding novel chemical entities);

PCA (Principal Component Analysis).

Results: COX-1 is a membrane-bound enzyme responsible for the oxidation of arachidonic acid to prostaglandins. An affinity fingerprint model (TRAP) has been constructed for COX-1 inhibition using known nonsteroidal antiinflammatory drugs (NSAIDs). The TRAP model was used to search for compounds from a chemical library for assay against COX-1. In the second round the TRAP model was refined by including 16 compounds that were found to be inactive against COX-1. Novel COX-1 inhibitors were discovered using the affinity fingerprints of 19 known NSAIDs. Three molecules were found that were in terms of IC_{50} values more potent than ibuprofen, a commonly used COX-1 inhibitor. These compounds were structurally distinct from those used to build the model and were discovered by testing only 62 library compounds. Fig. 1 shows the spatial relationships among the 19 NSAIDs (full circles), the 16 inactive compounds identified in the first round of compound selections (open circles), and the 3 active molecules (asterisks) identified in the second round of compound selections, in the two dimensions most important in selecting the compounds in the second round (as determined by principal components analysis).

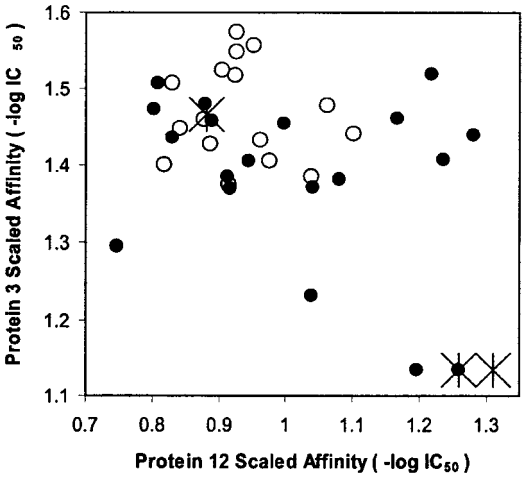

Fig. 1

The two active molecules in the lower-right-hand corner were selected by the interpolation model, while the active molecule in the upper left was chosen by the nearest-neighbor algorithm. The proposed method provides an alternative approach to extensive screening. The discovery of these novel lead compounds demonstrated the efficiency of the use of affinity fingerprints for identifying novel bioactive chemotypes from known drugs. The use of affinity fingerprints of known drugs as a starting point for compound selection is novel. (B. B.)

111/2005

Title: Efficient method for high-throughput virtual screening based on flexible docking. Discovery of novel acetylcholinesterase inhibitors.

Authors: Mizutani, M. Y.; Itai*, A.
Institute of Medicinal Molecular Design, Inc.
5-24-5 Hongo, Bunkyo-ku, Tokyo 113 – 0033, Japan.
E-mail: itai@immd.co.jp; Tel: 81-3-5689-4051; Fax: 81-3-5689-4054.

Source: J. Med. Chem. 2004, 47(20), 4818 – 4828.

Compounds:

a) 160000 Compounds, e.g., AChE ligand of type I;
b) Known noncovalent EChE inhibitors, e.g., donepezil, tacrine, physostigmine, galanthamine, huperzine A, decamethonium of type II, bis-THA, bis-HUPA.

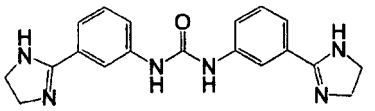

I

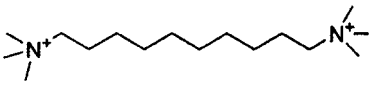

II

Biological material: Acetylcholinesterase form Torpedo californica (AChE).

Data taken from the literature:

Database [110000 commercially available compounds taken from the Available Chemicals Dictionary (ACD) and 47000 compounds taken from the Maybridge database];

Crystal structure [atomic coordinates of T. californica acetylcholinesterase in complex with decamethonium were taken from the Brookhaven Protein Data Bank (pdb code: 1ACL) resolved to 2.8 Å].

Computational methods:

Molecular modeling [the inhibitor and all water molecules were removed from the crystal structure of the acetylcholinesterase complex (1ACL), atomic charges were assigned to the protein atoms according to the default values of the program AMBER v5.0 by using the in house program PDBFIL, the protonation state of His in the catalytic triad in the active site gorge was properly determined, inside the ligand-binding region, a 3D grid with a regular interval of 0.4 Å and 42 H-bonding dummy atoms were generated by the program CALGRID, among those dummy atoms, six located at the bottom of cavity were selected and in the 3D database screening, ligands that could bind to these essential sites were searched];

ADA-M&EVE [a program for 3D automated ligand docking into receptors taking into account of the flexibility of the molecules by exploring the conformational space fully and continuously, parameters of the program can be adjusted allowing the fast computational screening of several

hundred thousand compounds, promising ligand candidates are selected according to various criteria based on the docking results and characteristics of compounds, a new tool, prior to 3D database screening EVE-MAKE, is used for automatically preparing the additional compound data, like assigning atomic types, atomic charges, conditions of bond rotation, etc., that are necessary for flexible docking calculation (details of the algorithm is given)].

Results: An efficient method is presented for high-throughput virtual screening based on flexible docking of ligands into protein receptors, allowing the identification of ligand candidates among a large number of flexible compounds in databases. The method, named ADAM&EVE, makes use of the automated docking method ADAM, which has already been reported. A virtual screening of about 160,000 commercially available compounds against the X-ray crystallographic structure of AChE has been performed yielding novel, promising AChE inhibitors. Among 114 compounds that could be purchased and assayed, 35 molecules with various core structures showed inhibitory activities with IC_{50} values below 100μM. Thirteen compounds displayed IC_{50} values between 0.5 and 10μM, and almost all their core structures were very different from those of known inhibitors. Fig. 1 shows the docking model of one of the identified AChE inhibitors of type I (thick lines), together with the complex crystal structures of the known inhibitor decamethonium (thick and dark lines) (hydrogens in the protein are omitted for clarity).

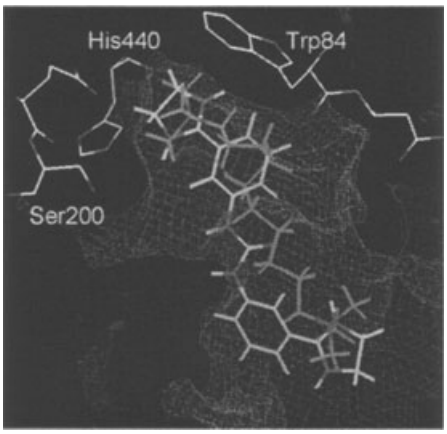

Fig. 1

The results demonstrated the effectiveness and validity of the proposed ADAM&EVE approach and proved to be a useful tool for the development of novel drugs to treat Alzheimer's disease. An advantages of ADAM&EVE is that docking is performed by covering all possible positions, orientations, and conformations of each compound effectively and rapidly. ADAM&EVE can screen a large number of flexible compounds in a practical time and also provides the docking modes.
(B. B.)

112/2005

Title: Successful virtual screening for a submicromolar antagonist of the neurokinin-1 receptor based on a ligand-supported homology model.

Authors: Evers, A.; Klebe*, G.

Institut für Pharmazeutische Chemie, Philipps-Universität Marburg

Marbacher Weg 6, D-35032 Marburg, Germany.

E-mail: klebe@mailer.uni-marburg.de; Tel: 49-6421-282-1313. Fax: 49-6421-282-8994.

Source: J. Med. Chem. 2004, 47(22), 5381 – 5392.

Compounds:

a) CP-96345 of type I as shown in Fig. 1;
b) 7 NK1 ligands, e.g., ASN-1377642 of type II;
c) 827000 Database compounds.

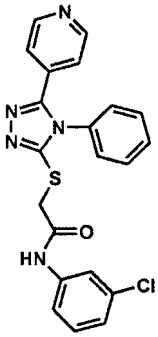

II

Biological material:

a) Neurokinin-1 (NK1), a member of the family of G-protein-coupled receptors (GPCRs);
b) Bovine rhodopsin.

Data taken from the literature:

Crystal structure	(atomic coordinates of rhodopsin were determined by X-ray diffraction techniques);
Crystal	[atomic coordinates CP-96345 were determined by X-ray diffraction techniques (CSD refcode: LEWCUL)];
Database	(a molecular database of 827000 compounds was assembled from seven different databases for virtual screening purposes).

Computational methods:

Docking	[virtual screening of the molecule database has been performed in a stepwise fashion, with a "hybrid" protein- and ligand-based computational approach, using Selector, Unity, and FlexX-Pharm employing several hierarchical filters of increasing complexity with respect to their computational requirements, (only compounds with up to seven rotatable bonds and a molecular mass of less than 450 Da have been considered)];
FlexX-Pharm	(program for automatic protein-ligand docking based on incremental construction without manual intervention, the program allows the incorporation of constraints derived from a pharmacophore hypothesis);
MOBILE	(MOdeling Binding sites Including Ligand information Explicitly is an approach which models proteins by homology considering information about bound ligands as restraints, thus resulting in more relevant geometries of protein binding sites).

Results: The family of GPCRs represents one of the most relevant target families in small-molecule drug design. In this study a successful virtual screening for a submicromolar antagonist of the neurokinin-1 receptor has been performed based on a ligand-supported homology model of the NK1 receptor based on the high-resolution X-ray structure of rhodopsin. The homology model of the NK1 receptor has been

generated using the novel MOBILE approach developed by the authors. For the building the NK1 receptor, the antagonist CP-96345 was used to restrain the modeling. The quality of the derived model was tested by exploring its ability to accommodate known NK1 antagonists from structurally diverse chemical classes. On the basis of the generated model and its interaction with known NK1 antagonists a pharmacophore model was derived which guided the 2D and 3D database search with UNITY. In a following step, the selected hits were docked into the modeled binding pocket of the NK1 receptor. Finally, seven ligands were selected for biochemical testing, yielding one compound (ASN-1377642) displaying affinity in the submicromolar range. Fig. 1 shows the structure-based pharmacophore hypothesis, with the docked ASN-1377642, where the H-bond interaction between the NH_2 of the terminal amide group of Gln^{165} (light ball) sphere) and a corresponding H-bond acceptor (black ball in the middle) is considered essential for all NK1 antagonists, and the sites for aromatic moieties within the aromatic ring are indicated by large spheres.

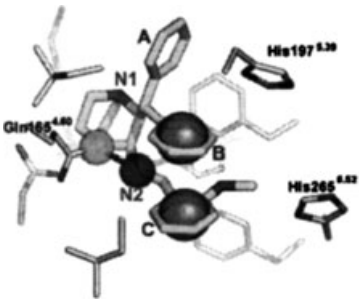

Fig. 1

The H-bond formed with Gln^{165} was found to be an important binding determinant. It was suggested that ligand-supported homology models of GPCRs may be used as effective tools for structure-based drug design.
(B. B.)

Molecular Graphics

113/2005

Title: Structure-activity relationships and molecular modelling of 5-arylidene-2,4-thiazolidinediones active as aldose reductase inhibitors.

Authors: Maccari*, R.; Ottaná, R.; Curinga, C.; Vigorita, M. G.; Rakowitz, D.; Steindl, T.; Langer, T.

Dipartimento Farmaco-chimico, Facoltá di Farmacia, Universitá di Messina

Viale SS. Annunziata, I-98168 Messina, Italy.

E-mail: rmaccari@pharma.unime.it; Tel.: 39-90-676-6406; Fax: 39-90-355-613.

Source: Bioorg. Med. Chem. 2005, 13(8), 2809 – 2823.

Compounds:

a) 19 Compounds of type I, where R^1 = H, CH_2COOCH_3, CH_2COOH, $CH_2CH{=}CHCOOCH_3$, $CH_2CH{=}CHCOOH$; R^2 = 3-Ph-O-Ph, 3-BzO-Ph, 4-Ph-Ph, α-naphthyl, 3-HO-Ph, 3-NH_2-Ph, 4-NH_2-Ph, 3-NO_2-Ph, 4-NO_2-Ph, 4-Ph-O-Ph, 4-Ph-Ph, 4-HO-Ph;

b) Idd384 of type II;

c) Sorbinil and ponalrestat.

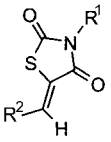

I

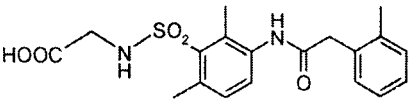

II

Biological material: Aldose reductase (EC 1.1.1.21, ALR2).

Data taken from the literature:

Crystal structure — [atomic coordinates of ALR2 complexed with the inhibitor idd384 of type III were taken from the Brookhaven Protein Data Bank (pdb code: 1EL3)].

Data determined:

IC_{50} — [concentration of the test substance (μM) required for 50% inhibition of ALR2, or% inhibition at the given concentration].

Computational methods:

Molecular modeling — [the molecular structures were built using the Catalyst v4.7 software package and the Cerius2 software package for docking, all the compounds used in this study were built using the 2D-3D sketcher of the program Catalyst, a representative family of conformations was generated for each molecule using the poling algorithm and the "best quality conformational analysis" method, and employing the CHARMm force field, the docking approach was carried out with the tool LigandFit implemented in the Cerius 2 software package was used for the docking and scoring procedure of the ligands into the ALR2 receptor, the final docked pose of Idd384 was found to be in good agreement with the orientation of the ligand in the crystal structure (1EL3), calculations were performed using the force field the compounds were rigidly docked keeping all parameters of interaction energy minimization, rigid body minimization and site partition at their default values, a final energy minimization of the ligands in the protein followed the fitting process, prioritization of the docked ligand orientations was achieved employing all seven scoring functions in Cerius2, using the predefined settings, finally a consensus score value was calculated, investigation of the best 100 poses (according to their consensus score) resulted in 19 different orientations of the selected ARIs according to the degree of superimposition onto Idd384];

Catalyst — [computer program for automatic generation of pharmacophore models for a training set of molecules specifying the relative alignments and active conformations of the ligands consistent with the binding to a common receptor site, the pharmacophore model (hypothesis) consists of a collection of features necessary for the biological activity of the ligands ar-

ranged in 3D space, the common ones being hydrogen bond acceptor, hydrogen bond donor, and hydrophobic features].

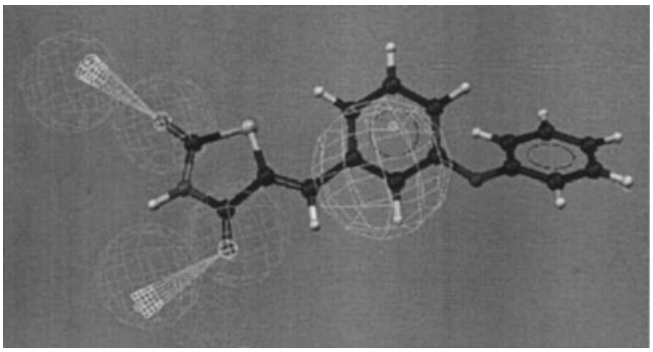

Fig. 1

Results: ALR2 is an aldo-keto reductase involved in the development of degenerative long-term complications of diabetes mellitus. In this study QSAR analysis and molecular modelling of the compounds of types I and II ALR2 inhibitors was performed. The substitution pattern on the 5-arylidene moiety and on N-3 was varied. The introduction of an additional aromatic ring or an H-bond donor group on the 5-benzylidene ring enhanced ALR2 inhibitory potency. The presence of a carboxylic anionic chain on N-3 was found to be an important, although not essential, structural requirement for high ALR2 inhibitory potential. The length of this carboxylic chain was critical and acetic acids with $R = CH_2$ COOH were the most effective inhibitors among the tested derivatives, showing higher inhibitory potency than that of sorbinil and similar to that of ponalrestat. Molecular docking simulations into the ALR2 active site agreed with the in vitro IC_{50} inhibition data. Fig. 2 shows the compound of type I, with $R^1 = H$, $R^2 = 3$-Ph-O-Ph (Ia) mappen onto the derived Catalyst pharmacophore model, where the cages drawn with thin and thick lines denote H-bond acceptor and lipophilic region, respectively.

Fig. 2 shows the superposition of docked structures of compounds of type I with $R^1 = CH_2COOCH_3$, $R^2 = 3$-Ph-O-Ph (thick lines) and type I with $R^1 = CH_2COOH$, $R^2 = 3$-Ph-O-Ph (dubble lines) with the bound conformation structure of Idd384 (intermediate lines).

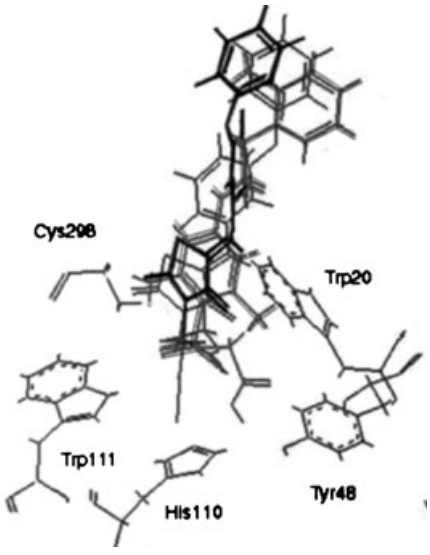

Fig. 2

The results allowed the rationalization of the observed structure-activity relationships and provided a pharmacophoric model for the studied class of AR inhibitors.
(B. B.)

114/2005

Title: The use of a pharmacophore model for identification of novel ligands for the benzodiazepine binding site of the $GABA_A$ receptor.

Authors: Kahnberg, P.; Howard, M. H.; Liljefors, T.; Nielsen, M.; Nielsen, E. Ø.; Sterner, O.; Pettersson*, I.
Protein Structure, Novo Nordisk A/S
Novo Nordisk Park, DK-2760 Måløv, Denmark.
E-mail: inpe@novonordisk.com; Tel.: 45-4443-4506; Fax: 45-4466-3450.

Source: J. Mol. Graphics Modell. 2004, 23(3), 253 – 261.

Compounds:

a) 38 Flavone derivatives of type I, where $R^1 = H$, NH_2, OCH_3, NO_2; $R^2 = H$, NO_2, CH_3, OCH_3, $CO_2CH(CH_3)_2$, CO_2CH_3, $CO_2CH_2CH(CH_2CH_3)_2$, $O(CH_2)_3CH_3$, NH_2; $R^3 = H$, OH, NO_2, CH_3, NH_2; $R^4 = H$, OH, NO_2, BENZO; $R^5 = H$, CH_3, Br, NO_2, C_2H_5, $(CH_2)^2CH_3$, $CH(CH_3)_2$, OCH_3; $R^6 = H$, OH; $R^7 = H$, CH_3; X = O, S; Y = C, N;
b) 11 Hit compounds from database searches, e.g., type II;
c) [^{3}H]-flumazenil, [^{3}H]-Ro 15 – 1788.

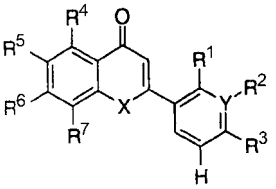

I

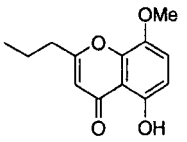

II

Biological material: Benzodiazepine binding site of the $GABA_A$ receptor in rat cortical membranes.

Data taken from the literature:

Compounds: [compounds retrieved from thr Maybridge and Available Chemicals Dictionary (ACD) databases].

Data determined:

K_i: [Michaelis inhibition constant (nM) representing the affinity of the substrate to displace the labeled ligands at the $GABA_A$ receptor].

Computational methods:

Molecular modeling: [conformational analysis and conformational analyses of hits from the database searching were performed using the MMFF94s force field and the Monte Carlo multiple minimum (MCMM) method implemented in the MacroModel v7 program, the calculations were performed in aqueous solution using the Generalized Born/solvent accessible surface area (GB/SA) dielectric continuum solvation model implemented in the MacroModel program, energy minimizations were carried out employing

the truncated newton conjugate gradient (TNCG) algorithm in MacroModel];

Catalyst [computer program for automatic generation of pharmacophore models for a training set of molecules specifying the relative alignments and active conformations of the ligands consistent with the binding to a common receptor site, the pharmacophore model (hypothesis) consists of a collection of features necessary for the biological activity of the ligands arranged in 3D-space, the common ones being hydrogen bond acceptor, hydrogen bond donor, and hydrophobic features].

Results: A Catalyst pharmacophore model has been developed for the identification of novel ligands for the benzodiazepine binding site of the $GABA_A$ receptor complex. The derived Catalyst model has been validated by using a set of 38 flavonoids with varying affinities for the benzodiazepine receptor and has been used as a search query in databases to find novel lead compounds. Fig. 1 shows the compound of type II mapped to the Catalyst pharmacophore with two hydrogen bond acceptors (A), one hydrogen bond donor (B) and two hydrophobic features (C), shape (D) and five exclusion spheres (E).

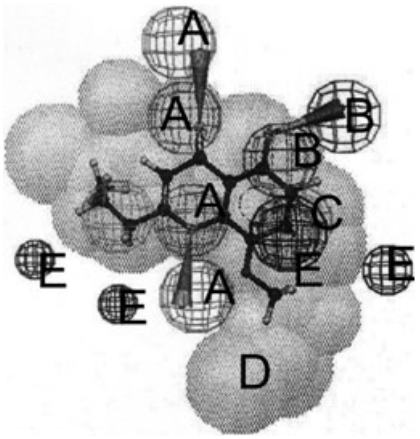

Fig. 1

Five of the hits from the database searching were tested against the $GABA_A$ receptor. Two of the compounds displayed K_i values in the lower milimolar range. The compound showing the highest potency in-vitro showed an affinity of 121 nM, a viable candidate for further optimization. The false positive ligands with $K_i > 10$ mM affinities have been analysed in terms of conformational energy penalties and possibilities for hydrogen bond interactions. The pharmacophore has been validated by identifying active compounds with a core structure different from the compounds used to generate the pharmacophore. Post-processing of the Catalyst hits in terms of hydrogen bond distances to hydrogen bonding pharmacophore elements in the search query is shown to be an efficient way of focusing the hit list.
(B. B.)

115/2005

Title: Homology modelling and binding site mapping of the human histamine H1 receptor.

Authors: Kiss, R.; Kovári, Z.; Keserü, G. M.

Department of Computer Assisted Drug Discovery, Gedeon Richter Ltd.

H-1475, Budapest 10, P. O. Box 27, Hungary.

E-mail: gy.keseru@richter.hu; Tel.: 36-1-431-4605; Fax: 36-1-432-6002.

Source: Eur. J. Med. Chem. 2004, 39(11), 959 – 967.

Compounds:

a) Mepyramine of type I and structurally analogous H1 antagonists: desloratidine, loratidine, chlorpheniramine, tripolidine, tripelennamine, chlorcyclizine, chloropyramine, diphenhydramine;
b) 9 Tricyclic H1 antagonists: phenothiazine, doxepin, loratadine, promethazine, olopatadine, desloratadine, chlropromazine, epinastine, ketotifen;
c) 4 Zwitterionic H1 antagonists: acrivastine of type II, cetirizine, fexofenadine, olopatidine;

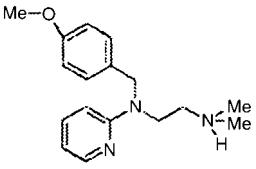

I

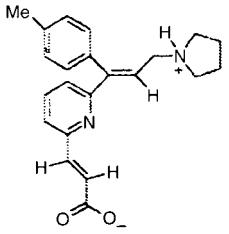

II

Biological material:

a) Human histamine H1 receptor (HHR1), a G-protein coupled receptor containing seven transmembrane α helices;
b) Bovine rhodopsin.

Data taken from the literature:

Crystal structure [atomic coordinates of the bovine rhodopsin crystal structure were taken from the Brookhaven Protein Data Bank (pdb code: 1F88)].

Computational methods:

Molecular modeling [comparative sequence analysis between HHR1 and bovine rhodopsin was performed using the program Clustal W the automatic sequence alignment was followed by manual adjustment, six initial HHR1 models were built by MODELLER v4 using the derived sequence alignment and the bovine rhodopsin crystal structure, the main geometric parameters of the models were determined by PROCHECK, one model was chosen for further investigations, which possessed on average the most favourable features, the selected model was subjected to a series of tests for its internal consistency and reliability, backbone conformation was evaluated by the inspection of the Psi/Phi Ramachandran plot obtained from PROCHECK analysis, the PROSA test was applied to check for energy criteria in comparison with the potential of mean force derived from a large set of known protein structures, packing quality of the homology model was investigated by the calculation of WHATIF Quality Control value, the derived homology model of HHR1 was used for docking antagonists into the binding site suggested by site-directed mu-

tagenesis studies, the channel surfaces of the receptor model were identified using the Multi Channel Surfaces module as implemented in Sybyl v6.9 with a 1.4 A probe radius, a considerable cavity was found in the TM region of the receptor, in close proximity to the conserved Asp^{107}, which was supposed to be one of the most crucial residues of the ligand binding in HHR1, all docking calculations were performed by the genetic algorithm based flexible docking code, FlexiDock as implemented in Sybyl 6.9, varying the parameters of the GA program a high diversity of sampled configuration of genes was obtained allowing sufficient sampling of the conformational space available for ligands within the binding site];

GA (Genetic Algorithm is a stochastic optimization method that mimics the process of evolution by manipulating a collection of data structures called chromosomes).

Data calculated:

pK_a (negative logarithm of the acidic dissociation constant of acrivastine were calculated by CompuDrug's Pallas v3.1 software).

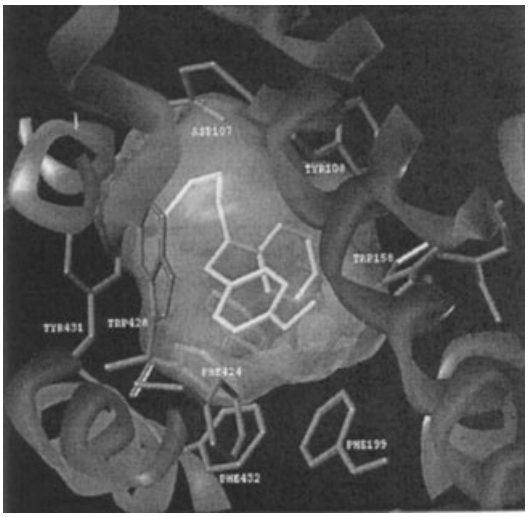

Fig. 1

Results: The H1 receptor is mainly responsible for the inflammatory effect of histamine, therefore, it is an attractive target for developing drugs against allergic rhinitis. In this study, homology modelling and binding site mapping of the human histamine H1 receptor has been performed using the high resolution structure of bovine rhodopsin as template. GA based docking calculations were employed to identify the role of several amino acid residues in the binding site involved in agonist or antagonist binding. Binding mode analyses of mepyramine, desloratidine, loratidine and acrivastine as ligands were carried out in order to rationalize their binding affinity. The binding site mapping established seven new potential aromatic interaction points Tyr^{108}, Phe^{184}, Phe^{190}, Phe^{199}, Phe^{424}, Trp^{428}, Tyr^{431} forming the lipophilic pocket of the antagonist binding pocket. (the residues Asp^{107}, Trp^{158}, Lys^{191}, Phe^{432}, Phe^{435} had been shown previously to play a role in antagonist binding). Fig. 1 shows the binding mode of mepyramine within the active site of HHR1. Residues that are important in forming the active site are dark band and labelled. Mepyramine, the docked ligand, is shown in light stick rendering within its translucent van der Waals surface.

Four known H1 antagonists were docked successfully into the developed HHR1 model, among others the zwitterionic acrivastine, which created two ionic interactions with Asp 107 and Lys 191. The docking results were in agreement with experimental site-directed mutagenesis data.
(B. B.)

116/2005

Title: Quantitative structure and aldose reductase inhibitory activity relationship of 1,2,3,4-tetrahydropyrrolo[1,2-a]pyrazine-4-spiro-3′-pyrrolidine-1,2′,3,5′-tetrone derivatives.

Authors: Ko, K.; Won*, Y.
Department of Chemistry, Hanyang University
Seoul 133 – 792, Korea.
E-mail: won@hanyang.ac.kr; Tel.: 82-2-2290-0944; Fax: 82-2-2299-0762.

Source: Bioorg. Med. Chem. 2005, 13(5), 1445 – 1452.

Compounds:

a) 4 Compounds of type I, containing one chiral center, where $R^2 = R^3 = H$; $R^4 = H$, CH_3, C_6H_5, C_6H_5-$(CH_2)_2$;
b) 26 Compounds of type II, containing one chiral center, where $R^1 = H$, F, Cl, Br, CH_3, CH_3O, CF_3, NO_2, NH_2.

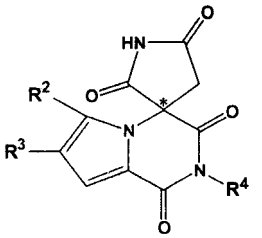

I

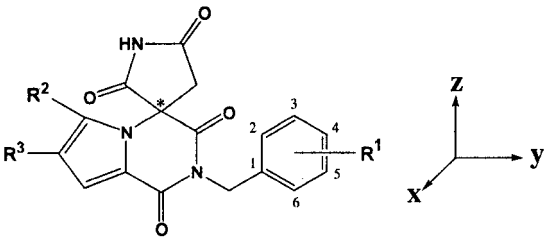

II

Biological material: Aldose reductase (AR), the first enzyme of the polyol pathway that catalyzes the conversion of D-glucose to D-sorbitol with NADPH.

Data determined:

IC_{50} [concentration of the test substance (pure S- or R-enantiomer) (μM) required for 50% inhibition of aldose reductase].

Computational methods:

Molecular modeling [conformational search and energy minimization of the compounds was performed using the Merck Molecular Force Field and the adopted basis Newton-Raphson minimization method, the molecular structure with the lowest energy of the compound of type I with R^1 = 4-F-4-Br, $R^2 = R^3 = H$, $R^4 = C_6H_3{-}CH_2{-}$ (SX3202) was close to that of AS-3201 docked in the active site of AR, the lowest energy structure of the (R)-enantiomers was the reasonable choice for the QSAR analyses];

GFA (Genetic Function Approximation for the generation of multiple QSAR models by evolving random initial models using a genetic algorithm);
LOO (Leave-One-Out cross-validation).

Data calculated:

Descriptors [physicochemical descriptors of the compounds have been calculated using the Cerius^2 package, including conformational, electronic, spatial, structural, thermodynamic, quantum mechanical, and molecular shape analysis descriptors, two sets of 78 molecular descriptors were obtained, one set for the (S)-enantiomer compounds (S-descriptors) and the other set for the R-enantiomer compounds (R-descriptors), the respective arithmetic mean values of R-descriptors and S-descriptors were also calculated (RS-descriptors)];
AlogP (logarithm of the partition coefficient in 1-octanol/water);
V_{NCOS} (non-common overlap steric volume);
μ_x, μ_y, μ_z (x, y, z components of the dipole moment);
α_{pol} (sum of the atomic polarizabilities);
TASA (the total hydrophobic surface area);
TPSA (total polar surface area);
PNSA1, PPSA1 (partial negative and positive, respectively, surface area);
PPSA2 (total charge weighted positive surface area);
PPSA3 (atomic charge weighted positive surface area);
DPSA1 (difference in charged partial surface areas: PPSA1 – PNSA1);
DPSA2 (difference in total charge weighted surface areas: $PPSA_2 - PNSA_2$);
Sy (length of molecules in the y-direction);
I_x, I_y (the x, y components of principal moment of inertia);
LOF (Friedman's lack of fit score for evaluating the models generated by GFA);
q^2 (cross-validated correlation coefficient).

Results: QSAR analysis of the AR inhibitory activity of type I compounds has been performed. The published assay data of 30 training compounds are related only for the racemic mixtures. As the physicochemical descriptors for the QSAR analysis were calculated for each of the (R)-enantiomers and (S)-enantiomers, a new "racemic" descriptor was devised as the arithmetic mean of the (R)-enantiomer descriptor and the (S)-enantiomer descriptor (RS-descriptor). The RS-equation was superior to its R- and S-counterparts in predicting the inhibitory activity of optically pure enantiomers as well as racemic mixtures. The RS-equation displayed larger regression coefficients with relatively small number of less intercorrelating terms than R- and S-equations. The five term RS-equation showed the following statistical parameters: $n = 27$, $r = 0.930$, $q^2 = 0.746$, $s = 0.144$, $F = 25.7$, $LOF = 0.349$. Fig. 1 shows the observed versus predicted activities of the compounds calculated using the five term RS-equation containing V_{NCOS}, TASA, $DPSA_1$, μ_x, S^2_y terms as descriptors.

The RS-equation revealed that the hydrophobic character of the benzyl moiety is the major contributing factor to the AR inhibitory activity. The contribution is governed by the polar descriptors, DPSA1 and μ_x. The equation also indicates that the bulky substitution at the R2 or R3 position is unfavorable for the inhibitory activity. The racemic QSAR model revealed that the hydrophobic character of the benzyl moiety was the major contributing factor to the AR reductase inhibitory activity and the polar surface area descriptors modulate the AR inhibitory activity. It was concluded that for AR inhibitors the RS-descriptors are suitable to perform QSAR analysis of the activity data assayed with racemates.
(B. B.)

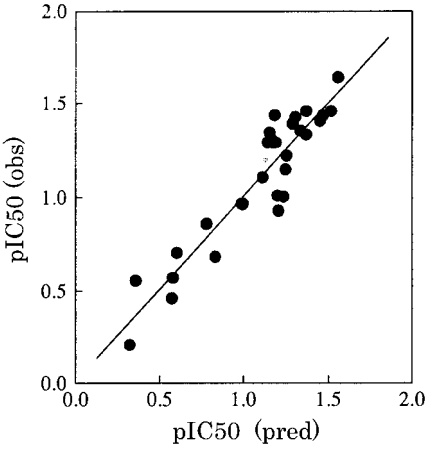

Fig. 1

117/2005

Title: Molecular design of cholesterols as inhibitors of DNA polymerase α.

Authors: Oshige, M.; Kuramochi, K.; Ohta, K.; Ogawa, A.; Kuriyama, H.; Sugawara, F.; Kobayashi, S.; Sakaguchi*, Kengo.

Frontier Research Center for Genome & Drug Discovery, Department of Applied Biological Science, Faculty of Science and Technology, and Faculty of Pharmaceutical Sciences, Tokyo University of Science

2641 Yamazaki, Noda-shi, Chiba-ken 278 – 8510, Japan.

E-mail: kengo@rs.noda.tus.ac.jp; Tel.: 81-471-24-1501/3409; Fax: 81-471-239767.

Source: J. Med. Chem. 2004, 47(20), 4971 – 4974.

Compounds:

a) Lithocholic acid (LCA) of type I;
b) 2-(cholesteryloxy)acetic acid of type II;
c) 2-(cholestanyl)acetic acid of type III;
d) 2-(stigmasteryl)acetic acid of type IV as they are shown in Fig. 1.

Biological material:

a) DNA polymerase α and β (pol.α and pol.β, respectively);
b) Human DNA topoisomerase II.

Data determined:

IC_{50} [concentrations of the test substance (μM) required for 50% inhibition of pol.α, pol.β, and human topoisomerase II].

Results: The triterpenoid structure is an attractive pharmacological target for the molecular design of DNA polymerase inhibitors. In this study, molecular design of cholesterols as inhibitors of DNA polymerase r has been performed. Among the tested 12 cholesterols the compounds of I – IV were shown to selectively affect only pol.α. As to the structural features, the presence of a carboxyl group at position 28 appeared to be essential for the inhibition of the pol.α activity acting by competing with the template-primer DNA and noncompetitively with the substrate. The relationships between the size/shape of active cholesterol analogues and the template-primer DNA-binding site of pol.α have been elucidated. In pol.β, LCA appears to be inserted into the pocket region comprising three amino acid residues (Lys^{60}, Leu^{77},

and Thr[79]). The size and the shape of LCA (12.43 Å × 11.35 Å × 4.83 Å), as shown in Fig. 1, exactly fit the three dimensions of the "a three-point interaction" between the small molecules and the pocket surface. Although the 3D structure of pol.α is still unknown, it is thought to have such pocket for LCA interaction.

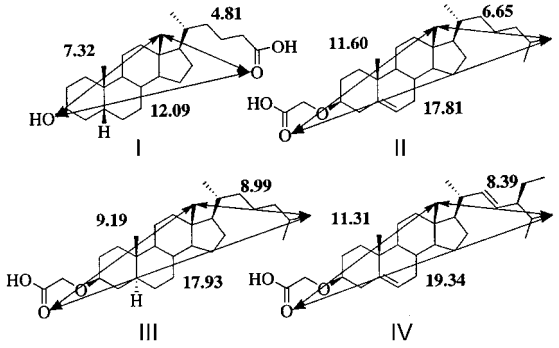

Fig. 1

Since the active compounds II-IV were almost same size (19 Å × 12 Å × 8 Å) (Fig. 1), the template-primer DNA-binding site of pol.α may also have "a three-point interaction" on the compound interactive surface. If so, the pocket in pol.α is larger to fit the size, 19 Å × 12 Å × 8 Å, than that in pol.β for LCA. The hydrophobic region (i.e., the backbone) and the hydrophilic region (i.e., carboxyl group or ketone group) in LCA are thought to bind to the hydrophobic sheet and the hydrophilic amino acids in the template-primer DNA-binding site of pol.β, respectively. The binding mode between the cholesterol and pol.α may be same as for the pol.β-LCA complex. The carboxyl group at position 28 appears to bind to the hydrophilic region in the pocket holding cholestrols on pol.α. Systematic studies using triterpenoid derivatives may facilitate the molecular design of inhibitors and the understanding of the mechanism on a molecular level, which eventually lead to the development of an anti-cancer agent.
(B. B.)

118/2005

Title: Comparing the conformational behavior of a series of diastereomeric cyclic urea HIV-1 inhibitors using the low mode. Monte Carlo conformational search method.

Authors: Parish*, C. A.; Yarger, M.; Sinclair, K.; Dure, M.; Goldberg, A.

Department of Chemistry, Hobart and William Smith Colleges

Geneva, NY 14456, USA.

E-mail: parish@hws.edu; Tel.: 1-315-781-3607; Fax: 1-315-781-3860.

Source: J. Med. Chem. 2004, 47(20), 4838 – 4850.

Compounds: Compound of type I as shown in Fig. 1.

Biological material:

a) Human immunodeficiency virus type-1 (HIV-1);
b) HIV-1 protease (HIV PR).

Data taken from the literature:

K_i [Michaelis inhibition constant (nM) representing the affinity of the cyclic ureas diastereomers of type I (RSSR, SRRS, RRRR, SSSS, RSRR, SRRR, RSRR, SRSS, RSRS) to HIV PR].

Computational methods:

Molecular modeling [force fields were validated by a comparison of the energetic ordering of the minimum energy structures on the AMBER*/GBSA(water), OPLSAA/GBSA(water) and HF/6-311G**/SCRF(water) surfaces];

Conformational searches [Low Mode:Monte Carlo (LM:MC) conformational search method was employed to generate conformational ensembles using MacroModel v7.2 suite of programs running on 800 MHz Athlon PCs under the RedHat LINUX 6.2 operating system, quantum calculations were performed with Jaguar v4.0 program, the LM:MC search method was employed in a 1:1 combination with the Monte Carlo (MC) search method to explore the potential energy surfaces of the stereoisomers of type I, each MC conformational search step varied a random number of torsional degrees of freedom between a minimum of two and a maximum of fourteen, where fourteen is the total number of variable torsion angles as shown in Fig. 1, LM frequencies corresponding to the 10 lowest eigenvectors were explored interconversion of ring structures was enabled using the ring-opening method of Still, starting structure chirality was preserved throughout the conformational searching, during the conformational search all structures were subjected to 1500 steps of the Truncated Newton Conjugate Gradient minimization method, ensembles generated for each of the 10 stereoisomers were grouped into geometrically similar families using the XCluster 80 program calculating the pairwise distance between each structure, in either torsional or Cartesian space, and partitioned the conformations into geometrically similar subsets in an agglomerative, hierarchical fashion].

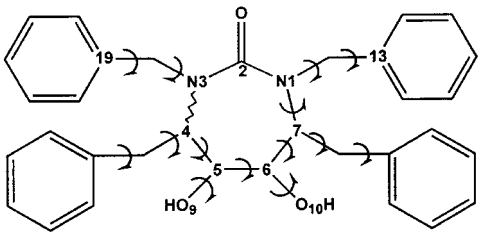

Fig. 1

Results: The conformational flexibility of a series of diastereomeric cyclic urea HIV-1 inhibitors was compared using the LM:MC conformational search method. It was found that the energetic ordering of the minima on the OPLSAA/GBSA(water) surface was in better agreement with the quantum calculations than the ordering on the AMBER*/GBSA(water) surface. An ensemble of low energy structures was generated using OPLSAA/GBSA(water) and applied to compare the molecular shape and flexibility of each diastereomer to the experimentally determined binding affinities and crystal structures of closely related systems. The diastereomeric solution-phase energetic stability, conformational rigidity and ability to adopt a chair conformation correlated significantly with experimental binding affinities. Rigid body docking indicated that all of the diastereomers adopted solution-phase conformations suitable for alignment with the HIV PR, and inhibitors with higher binding affinities (RSSR, RSRR and RSRR) were more precisely oriented for optimal interaction than inhibitors with low binding affinities (RSRS, RRRR and

RRSS). Fig. 2 shows representative structures of the two conformational families of RSRR.

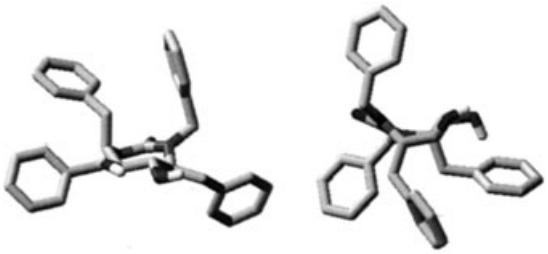

Fig. 2

The LM:MC conformational search method was capable to exhaustively search the OPLSAA/GBSA(water) surface and to identify the ensemble of all low lying structures of a series of diastereomeric cyclic urea HIV PR inhibitors. Analysis of each ensemble indicated that inhibitors with higher binding affinities were generally more rigid and were in the proper shape for optimal interaction with the protease active site. The ability to adopt a chair conformation encouraged ring substituents to adopt optimal binding orientations. The solvation free energy, as approximated by the GBSA energies, did not correlate to the binding affinity. The study indicated that N substitution plays an important role in orienting the substituents for optimal interaction with the active site.
(B. B.)

Programs, algorithms

119/2005

Title: A docking score function for estimating ligand-protein interactions. Application to acetylcholinesterase inhibition.

Authors: Guo, J.; Hurley, M. M.; Wright, J. B.; Lushington*, G. H.

Molecular Graphics and Modeling Lab, University of Kansas, Lawrence, Kansas 66045, USA.

E-mail: glushington@ku.edu; Tel.:1-785-864-1140; Fax: 1-785-864-5326.

Source: J. Med. Chem. 2004, 47(22), 5492–5500.

Compounds: 69 Structurally divers compounds, e.g., 22 compounds of type I, where R^1 = H, CH_3, OCH_3; R^2 = H, OCH_3, $NHCOCH_3$, $NHSO_2Ph$, -4-morpholino, NH_2, Br, CN, $CONH_2$; R^1 and R^2 together = $-CH_2CH_2CONH-$, $-HCOCH_2-$, $-N(CH_3)CONH_2-$; R^3 = H, OCH_3; R^2 and R^3 together = $-NHCOCH_2-$; X = $-(CH_2)_2-$, $-(CH_2)_3-$, $-OCH_2-$, $-NHCH_2-$, $-O-$, $-S-$, $-CH=CH-$, $-NH-$.

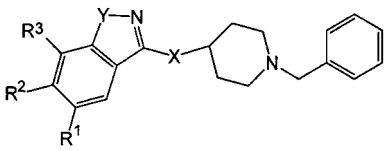

I

Biological material: Human acetylcholinesterase (hAChE).

Data taken from the literature:

Datasets (69 structurally diverse compounds with IC_{50} data measured with hAChE assay were selected for training and testing the scoring function, the activity among these compounds ranged from IC_{50} = 0.33 to 30000 nM);

Crystal structure [atomic coordinates of hAChE (pdb code: 1B41) and Torpedo californica AChE (tcAChE) (code: 1EVE) that includes the cocrystallized E2020 inhibitor].

Data determined:

IC_{50} [concentration of the test substance (nM) required for 50% inhibition of hAChE].

Computational methods:

Molecular modeling [protein modeling and docking was performed in Sybyl environment, geometry optimizations were carried out in MOE using the MMFF94 force field, a genetic algorithm (GA) was used in searching the binding conformation of flexible ligands, using the default parameters in GOLD, the scoring methods included empirical methods such as ChemScore, FlexXscore, and G Score, and knowledge based methods such as PMF score and DrugScore, MLR was used to obtain a consensus score from these methods, the selected conformations were used to fit an interaction field whose form, basically a variant of the comparative binding energy (COMBINE) method, the statistic analysis was performed using PLS analysis];

GOLD [flexible protein-ligand docking program featuring a (i) genetic algorithm methodology for protein docking; (ii) full ligand and partial protein flexibility; (iii) energy functions partly based on conformation and non-bonded contact information from the Cambridge Structural Database (CSD)].

MLR (Multivariate Linear Regression analysis);

PLS (Partial Least Squares projections to latent structures analysis performed using SIMCA-P);

LOO (Leave-One-Out cross-validation).

Data calculated:

rmsd [root mean square deviation (Å) of the position of the corresponding atoms of two superimposed molecular structures];

q^2 (cross-validated correlation coefficient).

Results: Inhibition of AChE is an important research topic because of its wide range of associated health implications. In this study a receptor-specific docking score function has been developed for estimating ligand-protein interactions and applied to the study of hAChE inhibition. The proposed method utilizes a statistically trained weighted sum of electrostatic and van der Waals (VDW) interactions between ligands and receptor residues. The consensus score was built over the 53-molecule set, yielding a weighted sum over five commercially available scoring functions (Eq. 1),

$$pIC_{50} = 0.05682\ \text{Chemscore} - 0.00499\ \text{Drugscore} - 0.03582\ \text{Flexscore} - 0.01232\ \text{PMFscore} + 7.62820 \quad 1)$$

where Chemscore, Drugscore, Flexscore, Gscore, and PMFscore refer to computed affinities from the Chem-Score, DrugScore, FlexX score, G Score, and PMF score methods, respectively. A strong correlation was found within the 53 training set ligands between the computed and experimental

inhibition constants ($R^2 = 0.89$). LOO cross-validation indicated high predictive power ($q^2 = 0.72$), and analysis of a separate 16-compound test set also yielded very good correlation with experiment ($R^2 = 0.69$). Fig. 1 shows the plot of the predicted versus observed pIC_{50} values for the training set.

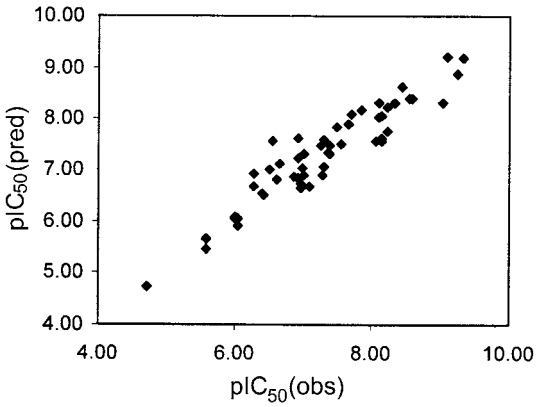

Fig. 1

Scoring function analysis allowed the identification and characterization of important ligand-receptor interactions. A list of those residues has been produced that made the most important electrostatic and VDW contributions within the main active site, gorge area, acyl binding pocket, and peripheral site. The results of these analyses were consistent with X-ray crystallographic and site-directed mutagenesis studies. Comparison with other scoring methods and consensus scoring indicated the high effectiveness and predictability of this method.
(B. B.)